2020

Archaeosine Modification of Archaeal tRNA - A Role in Structural Stabilization

Ben Turner
Portland State University

Brett w. Burkhart
Colorado State University - Fort Collins

Katrin Weidenbach
University of Kiel

Robert Ross
University of Cincinnati

Patrick A. Limbach
University of Cincinnati

See next page for additional authors

Citation Details

Published as: Turner, B., Burkhart, B. W., Weidenbach, K., Ross, R., Limbach, P. A., Schmitz, R. A., ... & Iwata-Reuyl, D. (2020). Archaeosine Modification of Archaeal tRNA: Role in Structural Stabilization. Journal of Bacteriology, 202(8).

Archaeosine modification of archaeal tRNA – a role in structural stabilization

Ben Turner[1], Brett W. Burkhart[2], Katrin Weidenbach[3], Robert Ross[4], Patrick A. Limbach[4], Ruth A. Schmitz[3], Valérie de Crécy-Lagard[5], Kenneth M. Stedman[6], Thomas J. Santangelo[2], and Dirk Iwata-Reuyl[1]*

[1] Department of Chemistry, Portland State University, Portland, Oregon, 97201, USA
[2] Department of Biochemistry and Molecular Biology, Colorado State University, Fort Collins, Colorado, 80523, USA
[3] Institute of General Microbiology, University of Kiel, D-24118, Kiel, Germany
[4] Department of Chemistry, University of Cincinnati, Cincinnati, Ohio, 45221, USA
[5] Department of Microbiology and Cell Science, University of Florida, PO Box 110700, Gainesville, Florida, 32611 USA
[6] Department of Biology, Portland State University, Portland, Oregon, 97201, USA
* To whom correspondence should be addressed. Tel: 1-503-735-5737; Email: iwatard@pdx.edu

ABSTRACT Archaeosine (G^+) is a structurally complex modified nucleoside found quasi-universally in the tRNA of Archaea and located at position 15 in the dihydrouridine loop, a site not modified in any tRNA outside of the Archaea. G^+ is characterized by an unusual 7-deazaguanosine core structure with a formamidine group at the 7-position. The location of G^+ at position 15, coupled with its novel molecular structure, led to a hypothesis that G^+ stabilizes tRNA tertiary structure through several distinct mechanisms. To test whether G^+ contributes to tRNA stability and define the biological role of G^+, we investigated the consequences of introducing targeted mutations that disrupt the biosynthesis of G^+ into the genome of the hyperthermophilic archaeon *Thermococcus kodakarensis* and the mesophilic archaeon *Methanosarcina mazei*, resulting in modification of the tRNA with the G^+ precursor 7-cyano-7-deazaguansine ($preQ_0$) (deletion of *arcS*) or no modification at position 15 (deletion of *tgtA*). Assays of tRNA stability from *in vitro* prepared and enzymatically modified tRNA transcripts, as well as tRNA isolated from the *T. kodakarensis* mutant strains, demonstrate that G^+ at position 15 imparts stability to tRNAs that varies on the overall modification state of the tRNA and the concentration of magnesium chloride, and that when absent results in profound deficiencies in the thermophily of *T. kodakarensis*.

IMPORTANCE Archaeosine is ubiquitous in archaeal tRNA where it is located at position 15. Based on its molecular structure it was proposed to stabilize tRNA, and we show that loss of archaeosine in *Thermococcus kodakarensis* results in a strong temperature sensitive phenotype while there is no detectable phenotype when lost in *Methanosarcina mazei.* Measurements of tRNA stability show that archaeosine stabilizes tRNA structure, but that this effect is much greater when present in otherwise unmodified tRNA transcripts than in the context of fully modified tRNA, suggesting that it may be especially important during the early stages of tRNA processing and maturation in thermophiles. Our results demonstrate how small changes in the stability of structural RNAs can be manifested in significant biological-fitness changes.

INTRODUCTION

Transfer RNA (tRNA) is notable for harboring a stunning diversity of post-transcriptional chemical modifications, typically representing ~10-20% of the nucleosides in a particular tRNA (1). To date, over 130 modified nucleosides have been structurally characterized (2,3), which vary from simple methylation of the base or ribose to extensive "hypermodification" of the canonical bases, the latter of which can result in radical structural changes and involve multiple enzymatic steps to complete. While we are still far from a comprehensive understanding of the roles of tRNA modification, it has become clear that modified nucleosides are integral to tRNA function at many levels, influencing translation (4-8), tRNA structure and stability (1,9-13), and regulatory events (14-16).

Among the most complex modifications known to occur in tRNA are the 7-deazaguanosine nucleosides archaeosine (G^+) (17) and queuosine (Q) (18) (Figure 1). Although both nucleosides share the core 7-deazaguanine structure, they are rigorously segregated with respect to phyla and location in the tRNA. Queuosine is ubiquitous throughout Bacteria and Eukarya (19) where it occurs specifically at the wobble position (20) in a subset of tRNAs (those coding for Tyr, His, Asp, and Asn). In contrast, archaeosine is present exclusively in the Archaea, where it is found in virtually all archaeal tRNAs at position 15 of the dihydrouridine loop (21), a site not modified in any tRNA outside of the Archaea; in at least a few species, G^+ is also present at position 13 (22).

Despite the observed phylogenetic segregation, G^+ and Q share a significant portion of their biosynthesis, and they remain the only modified nucleosides known for which a portion of the pathway occurs extrinsic to the tRNA, requiring the initial formation of a modified precursor base (23). All other modified nucleosides are formed exclusively via modification of a genetically encoded base in the RNA transcript. The pathway begins (Figure 1) with the conversion of GTP to dihydroneopterin triphosphate (H_2NTP; Bacteria, Archaea) or the cyclic monophosphate (H_2NcMP; Archaea) by the enzyme GCYH-IA in Bacteria (24) or GCYH-IB in Bacteria (25,26) and Archaea (27), steps shared with the pterin pathways. After hydrolysis of H_2NcMP (Archaea) by the enzyme MptB (28) the dihydroneopterin monophosphate (or triphosphate) is converted to carboxytetrahydropterin (CPH_4) through the action of QueD (29), followed by the QueE catalyzed ring contraction to 7-carboxy-7-deazaguanine (CDG) (30), and the formation of 7-cyano-7-deazaguanine ($preQ_0$) by QueC (31). $PreQ_0$ is the point of divergence in the bacterial and archaeal pathways, with $preQ_0$ serving as the substrate for the enzyme tRNA-guanine transglycosylase (aTGT in Archaea, also known as 7-cyano-7-deazaguanine tRNA-ribosyltransferase), which catalyzes the exchange of the genetically encoded guanine-15 for $preQ_0$ in archaeal tRNA. The $preQ_0$-modified tRNA is converted to G^+-modified tRNA by the action of either ArcS (32), QueF-L (33), or GAT-QueC (34), depending on the organism. In Bacteria $preQ_0$ is first reduced to $preQ_1$ (35) before being inserted into specific bacterial tRNA at position 34 (the wobble position) by a bacterial tRNA-guanine transglycosylase (bTGT) (23) and further elaborated to Q-modified tRNA (36-38). Eukarya lack the *de novo* pathway and instead scavenge queuine, the free base of queuosine, from the environment, and a eukaryal TGT (eTGT) inserts queuine directly into the relevant tRNA (39), again at position 34.

The location of queuosine in the anticodon of specific bacterial and eukaryotic tRNAs suggests a role in modulating translational fidelity and efficiency, and studies are consistent with such a role (40-44). Archaeosine's location at position 15, in the body of the tRNA, and its novel molecular structure led to a hypothesis that this modification functions (at least in part) to stabilize the structure of archaeal tRNA (17) via coulombic interactions of the positively charged formamidine group and the backbone phosphates in the vicinity. Notably, nucleotides 15 and 48 comprise the Levitt base-pair, a conserved structural motif in the core of all tRNA that is crucial for the overall structural integrity of tRNA. Computational studies revealed that the Levitt base-pair H-bonds are stronger in archaeosine-modified tRNA as compared to unmodified tRNA (45) due to the electron withdrawing effect of the formamidine moiety (45), an effect that mimicked metal ion coordination to N7 of guanine. Thus, two distinct mechanisms could be relevant to potential structural stabilization by G^+.

To test the hypothesis that G^+ serves to stabilize the structure of tRNA we investigated the role of archaeosine both *in vivo* and *in vitro*. If as proposed G^+ is important to tertiary structural stability of tRNA, this role would be especially critical in thermophilic organisms, where growth temperatures approach or exceed those needed to denature isolated tRNA, and G^+-defective mutants should exhibit, at minimum, a temperature sensitive phenotype. Therefore, we carried out targeted gene knockouts of two genes in the G^+ pathway in the hyperthermophile *Thermococcus kodakarensis* and investigated the consequences of these mutations on growth over a range of temperatures. As a complement we also generated a knockout strain in the mesophile *Methanosarcina mazei* resulting in a strain lacking G^+ and investigated its growth under a wide variety of growth conditions. To directly probe the structural impact of modification with $preQ_0$ or G^+ we investigated the thermal stability of tRNA possessing or lacking these modifications in the context of both fully modified tRNA isolated from *T. kodakarensis* strains as well as tRNA produced via *in vitro* transcription and modified with either $preQ_0$ or G^+ but lacking all other modifications.

We discovered that the genes of the G^+ pathway are non-essential in both *T. kodakarensis* and *M. mazei*, but deletion strains of *T. kodakarensis* are temperature sensitive as predicted, consistent with the results of a recent genome wide transposon mutagenesis screen (46) in which one of these genes (*tgtA*) was identified as important to thermophily. Additionally, we found that modification with G^+ imparts a modest but measurable stabilizing effect on tRNA that is most apparent in tRNA transcripts that are otherwise unmodified.

RESULTS

T. kodakarensis and *M. mazei* mutant construction

We targeted two genes encoding archaeosine biosynthetic proteins in the hyperthermophilic model archaeon *Thermococcus kodakarensis* for deletion from the genome. *TK0760* (*tgtA*) encodes a homologue of the archaeal tRNA-guanine transglycosylase (aTGT, UniProt Q5JHC0) while *TK2156* (*arcS*) encodes a homologue of archaeosine synthase (ArcS, UniPrpot Q5JHG7) (Figure 2, panels A and D, respectively); these enzymes catalyze the final, and only tRNA dependent, steps in the

biosynthesis of archaeosine (Figure 1). Beginning with strain TS559, markerless deletion of the entire coding sequence of *tgtA* was possible, as was the deletion of most of *arcS* (to the exclusion of the 23 bp that overlap with the divergent locus, *TK2155*). Deletion of each locus was confirmed by a series of diagnostic PCRs with purified genomic DNAs from each strain (Figure 2, panels B and E, respectively). Further confirmation of each deletion was provided by Southern blots of BspHI and BstEII digested preparations of genomic DNA from strains *T. kodakarensis* Δ*tgtA* and Δ*arcS,* respectively (Figure 2, panels C and F). For each locus, probes complementary to the target gene (probes 2 & 4, Figure 2) were unable to hybridize to any location on the genomes from the deletion strains, while probes complementary to adjacent sequences (probes 1 & 3, Figure 2) did hybridize to genomic fragments that were shorter in deletion strains than those derived from strain TS559. In both instances, the difference in size of the identified DNA fragment was consistent with the size of the target gene that was deleted.

To investigate the consequences of archaeosine loss in a mesophile, the *M. mazei* gene *MM1101* (*tgtA*) encoding aTGT (UniProt Q8PXW5) (47) was disrupted by the insertion of a puromycin-resistance (*pac*) cassette by homologous recombination (Figure 3, panel A). Three independent puromycin-resistant transformants were isolated and grew at 37 ˚C. The absence of the *tgtA* gene and presence of the puromycin resistance cassette was confirmed by both PCR and Southern hybridization (Figure 3, panels B and C, respectively).

Nucleoside analysis of bulk tRNA from the *T. kodakarensis* and *M. mazei* cell lines

To confirm that tRNAs in the mutant strains were appropriately modified, purified tRNA from each of the *T. kodakarensis* and *M. mazei* strains were subjected to nuclease digestion and dephosphorylation, followed by HPLC analysis of the resulting nucleosides. The tRNA from the three *T. kodakarensis* strains displayed the predicted pattern of modified nucleosides (Figure 4A); $preQ_0$-nucleoside and G^+ were absent from the *T. kodakarensis ΔtgtA* strain, and $preQ_0$ was present in the *T. kodakarensis ΔarcS* strain, with G^+ being present only in the wild-type strain. Similarly, only the tRNA from the wild-type *M. mazei* strain contained G^+ (Supplemental Figure 1).

To further address the modification status of the tRNA and confirm the peak assignments we analyzed the tRNA from the *T. kodakarensis* strains by LCMS (Figure 4B-D). Analysis of the nucleoside digests from the isolated tRNA from the *T. kodakarensis* cell lines confirmed the initial HPLC data with one exception; while no G^+ was detected in the tRNA digests from either the *T. kodakarensis ΔtgtA* or *ΔarcS* strains by HPLC, LCMS analysis was able to detect G^+ in the *T. kodakarensis ΔarcS* samples, which varied from 1.6 – 6.6% of the intensity of that for $preQ_0$-nucleoside (Figure 4D).

Temperature dependent growth of *T. kodakarensis* strains disrupted in archaeosine biosynthesis

Deletion strains in *T. kodakarensis* were constructed at 85 ˚C and we noted that colonies from strains deleted for *tgtA* or *arcS* were slightly smaller than colonies produced by TS559. It was clear that loss of archaeosine biosynthesis was not lethal, but it appeared that loss of archaeosine biosynthesis did hinder growth. To more accurately measure growth of each strain, we monitored the

optical densities of growing cultures, while varying the incubation temperature to identify any potential role for archaeosine modification at reduced (70 ˚C), optimal (85 ˚C) or elevated (95 ˚C) temperatures (Figure 5). *T. kodakarensis* can support two radically different metabolic strategies based on the availability of elemental sulfur (S˚) in the media, thus we monitored growth in the absence and presence of sulfur at three different temperatures.

While deletion of *tgtA* or *arcS* had minimal or essentially no effect, respectively, on growth of *T. kodakarensis* cultures at 70˚C (Figure 5, panels A and D), severe phenotypes were noted at elevated (95 ˚C) temperatures where neither deletion strain could support robust growth even after >30 hours incubation (Figure 5, panels C and F). Growth at the optimal temperature of 85 ˚C was more modestly compromised for strains deleted for *arcS* or *tgtA*, with growth more severely affected in the absence of sulfur (Figure 5, panels B and E), an observation that extended to growth of the *ΔarcS* strain at 70 ˚C.

Growth under diverse conditions of *M. mazei* strains disrupted in archaeosine biosynthesis

We tested three independent *M. mazei* mutants with insertions in the *tgtA* gene for growth under various conditions relative to wild-type *M. mazei*. Growth was indistinguishable between wild-type and mutants at reduced (25 ˚C), sub-optimal (30 ˚C), and optimal (37 ˚C) growth temperatures (Supplemental Figure 2). In order to test additional stress conditions the *M. mazei* strains were grown under multiple conditions that have previously been determined to induce a stress response (48). These included the presence of metals (e.g. copper and nickel), high salt, the absence of sulfide, or the presence of antimicrobials. In each case, no difference in growth between wildtype and mutants was detected (Supplemental Figure 3).

Thermal denaturation study of *in vivo* tRNA^{Gln} from *T. kodakarensis* and *in vitro* tRNA^{Gln} transcripts

To directly probe for a potential structural role for G^+ in tRNA we investigated the thermal denaturation of tRNA extracted from the *T. kodakarensis* strains by measuring the hyperchromicity at 260 nm upon denaturation. In these experiments the raw melt data was processed to obtain a differential melting profile (first derivative plot of dAbs/dT vs temperature), which allowed the apparent melting temperature (T_m) to be easily determined over a range of magnesium chloride concentrations, from 0 to 10 mM in a buffer of 10 mM sodium cacodylate (pH 7.0) and 100 mM NaCl. Although it was recently reported that unfractionated tRNA from a *T. kodakarensis* strain lacking G^+ exhibited a T_m 2 ˚C lower than unfractionated tRNA from the wild-type strain (46), we were unable to observe discernable differences in the denaturation profiles of unfractionated tRNA from our three strains (data not shown), so we chose to investigate the behavior of a specific tRNA isolated from these strains, and selected tRNA^{Gln} for further investigation.

The tRNA^{Gln} isoacceptors were purified from the *T. kodakarensis* strains utilizing an affinity approach (49) as detailed in the Materials and Methods. As with the unfractionated tRNA, the raw thermal denaturation data (Supplemental Figure 4) from the purified tRNA^{Gln} derived from the three strains was processed to obtain differential denaturation profiles (Figure 6). Surprisingly, the tRNA^{Gln} from the parental strain (TS559) containing G^+ at position 15, and the *ΔtgtA* strain containing G,

behaved almost identically (Figure 6). In the absence of Mg^{2+} both exhibit a slight shoulder at ~70 °C and a main transition (the T_M) at ~83 °C (Figure 6A). The T_M is similar for $tRNA^{Gln}$ from the *T. kodakarensis* Δ*arcS* strain (containing $preQ_0$), but there is also a distinct shoulder in the latter at ~64 °C (Figure 6A). At 100 μM Mg^{2+} the profiles for the $tRNA^{Gln}$ from the TS559 and *T. kodakarensis* Δ*tgtA* strains have lost the shoulder and exhibit a single well-defined T_M at 83 °C and 82 ˚C, respectively (Figure 6B). At the same Mg^{2+} concentration the differential plot for the $tRNA^{Gln}$ from the *T. kodakarensis* Δ*arcS* strain has coalesced into a very broad but asymmetric profile with the T_M at ~75 °C. At 10 mM Mg^{2+} the $tRNA^{Gln}$ from all three strains denature at a temperature beyond the 98 °C limit of the experiment (Figure 6C).

To investigate the potential role of G^+ in tRNA stability free from the effects of other modified nucleosides, we carried out thermal denaturation studies on tRNA produced through *in vitro* transcription and enzymatically modified to contain $preQ_0$ or G^+ at position 15. A tRNA transcript corresponding to *T. kodakarensis* $tRNA^{Gln}$(CUG) (with the 5' adenosine substituted for guanosine) was prepared from a duplex DNA template as described in the Materials and Methods. A portion of the $tRNA^{Gln}$ transcript was then reacted *in vitro* with recombinant aTGT (Figure 1) from *Methanocaldococcus jannaschii* (50) to replace the genetically encoded G at position 15 with $preQ_0$. A portion of the $preQ_0$-modified tRNA was then further reacted with recombinant *M. jannaschii* ArcS (32) to produce G^+-modified tRNA (Figure 1). Quantitation of $preQ_0$ incorporation and subsequent conversion to G^+ was carried out as described in the Materials and Methods, and the modification state of the tRNA confirmed by HPLC (Supplemental Figure 5).

Similar to our observations with $tRNA^{Gln}$ isolated from the *T. kodakarensis* Δ*tgtA* mutant, in the absence of magnesium the unmodified $tRNA^{Gln}$ transcript exhibited a shoulder in the differential thermal denaturation plot at ~70 ˚C along with a T_M of 84 °C (Figure 7A). In contrast, the effect of modification at position 15 on the $tRNA^{Gln}$ transcript was markedly different than that observed for the *in vivo* produced tRNA. The $preQ_0$- and G^+-modified $tRNA^{Gln}$ transcripts both exhibit a T_M significantly above that of the unmodified $tRNA^{Gln}$ at 88 and 89 ˚C, respectively. While both profiles also feature a shoulder - for the G^+-modified $tRNA^{Gln}$ transcript it is very distinct – these occur at a lower temperature (~67 ˚C) than the unmodified transcript. Notably, the T_M's for the modified transcripts are significantly higher than observed in the fully modified tRNA isolated from *T. kodakarensis.* In the presence of 100 μM $MgCl_2$ the T_M increases to ~86 ˚C for the unmodified transcript and to 90 ˚C for the G^+-modified transcript, while the T_M remains unchanged at 88 ˚C for the $preQ_0$-modified transcript (Figure 7B). The shoulder persists in the profiles for all three tRNAs with an increase of 1-2 ˚C. In the presence of 10 mM $MgCl_2$ the denaturation is not complete for any of the tRNAs at 98 ˚C (Figure 7C), the highest temperature reached in the experiment.

DISCUSSION

Archaeosine is a structurally complex modified nucleoside found in the tRNA of Archaea, and recently has been discovered in viral and bacterial DNA (51). The proposals that G^+ functions to

stabilize tRNA tertiary structure (17,45) prompted us to investigate this putative role *in vivo* through the construction and phenotypic characterization of *T. kodakarensis* and *M. mazei* strains that were disrupted in G^+ biosynthesis, and *in vitro* by directly measuring the thermal stability of tRNA in the presence and absence of G^+.

Our observation of temperature-sensitivity in *T. kodakarensis* lacking G^+ is consistent with a role in structural stabilization of the tRNA by G^+, and mirror the results of a recent transposon mutagenesis study (46) in *T. kodakarensis*, which reported that disruption of the *tgtA* gene and loss of G^+ modification was accompanied by loss of thermophily. Importantly, because we also observed this phenotype in the *ΔarcS* mutant, which possesses $preQ_0$-modified tRNA, the loss of thermophily can be conclusively attributed to the unique physicochemical properties of G^+. Interestingly, we observed no phenotypic differences between the wild-type and G^+ deficient strains of the mesophile *M. mazei* under a range of growth conditions including growth at sub-optimal temperatures, while in *Haloferax volcanii*, also a mesophile and the only other organism in which loss of G^+ has been investigated, loss of G^+ was accompanied by cold-sensitivity (52). Although both hot and cold tolerances can be rationalized by tRNA structural effects, the nature of these effects are typically in opposition to one another, with heat tolerance being associated with increasing structural rigidity and cold tolerance on relaxing structural rigidity, so the observation of both phenotypes accompanying loss of G^+ is intriguing, and may be due to the significant differences in the *in vivo* environments, most notably the very high salt concentrations in halophilic species.

While the presence or absence of G^+ in $tRNA^{Gln}$ isolated from *T. kodakarensis* had minimal impact on the overall stability of the otherwise fully modified tRNA, its presence had a significant effect on the stability of the tRNA transcripts, with the stabilizing effect manifested in a 4-5 ˚C increase in the T_m depending on the concentration of $MgCl_2$. The magnitude of the observed change in T_m is of the order of other modifications that have been characterized as structurally important (13), and approaches that for ribothymidine at position 54 of *E. coli* $tRNA^{Met}$ (53), which contributes 6 ˚C to the T_m of the tRNA. The fact that the effect is most pronounced for *in vitro* transcribed tRNA, which is devoid of other modifications, suggests that this role may be most important in the early stages of folding and processing the nascent transcript. This interpretation is consistent with kinetic studies of aTGT, which revealed that the best substrates for the enzyme are unstructured RNAs (54,55). While disruption of tRNA folding and/or processing due to the absence of G^+ can easily account for the growth defects observed at higher temperatures for both *T. kodakarensis* mutants, we cannot rule out the possibility that otherwise fully modified tRNAs respond differentially to the presence or absence of G^+, and some tRNA (other than $tRNA^{Gln}$) may exhibit more significant decreases in thermal stability in the absence of G^+.

Surprisingly, deletion of *arcS* in *T. kodakarensis* did not completely abolish G^+ biosynthesis, with the knockout strain displaying small amounts of G^+ up to 6.6% that of $preQ_0$-nucleoside. While this low level of G^+ was not significant in terms of the growth or thermal denaturation experiments, it does lead to the question of how G^+ is formed in this mutant. The formation of G^+ from $preQ_0$-modified tRNA is the only step in the G^+ pathway in which multiple non-homologous enzymes have been

discovered that catalyze the same transformation (Figure 1); in addition to ArcS, the enzymes QueF-L (33,34) and GAT-QueC (34) have also been shown to catalyze the formation of G^+ from $preQ_0$-modified tRNA. While a number of organisms possess more than one of these enzymes (34), neither QueF-L or GAT-QueC is present in *T. kodakarensis* (34). However, a number of organisms that possess genes encoding the rest of the G^+ pathway lack genes encoding any of the three known enzymes that form G^+ (reference (34) and Supplementary Table 1), so it is likely that there exists at least one more enzyme responsible for G^+ formation, and it may be present in *T. kodakarensis*.

Overall, both the *in vivo* results with *T. kodakarensis* and the *in vitro* biophysical studies (ours and those of Orita et al. (46)), support the original proposal that G^+ is important for thermostability of archaeal tRNA (17), and demonstrate how small changes in the stability of structural RNAs can be manifested in significant biological-fitness changes. Nevertheless, the near ubiquity of G^+ in the Archaea (it is absent only in *Haloquadratum walsbyi*), the majority of which are not thermophiles, argues for a more fundamental and universal role, but the absence of any distinct phenotypes in the *M. mazei* Δ*tgtA* mutant suggest that this role is a subtle one.

MATERIAL AND METHODS

General

Buffers and salts of the highest grade available were purchased from Sigma-Aldrich unless otherwise noted. DEPC (diethylpyrocarbonate) treated water was used for all solutions used for RNA related assays (56). All buffers and solutions were otherwise prepared with Millipore MQ grade water. Dithiothreitol (DTT), isopropyl-β-D-thiogalacto-pyranoside (IPTG), kanamycin sulfate, DEPC and ampicillin were purchased from RPI Corporation. [8-^{14}C]-guanine was purchased from PerkinElmer. Adenosine, guanosine, ATP, GTP, UTP, CTP were all purchased from Sigma-Aldrich. Nickel-nitrile tetraacetic acid (Ni^{2+}-NTA) was purchased from Qiagen and Sigma-Aldrich. Whatman GF-B filter disks were purchased from Fisher Scientific. Amicon centrifugal concentrators were from MilliporeSigma. Dialysis tubing was obtained from ThermoFisher Scientific. Plasmid Mini-Kits were from Fermentas and Qiagen. Oligonucleotides were obtained from IDT or Operon. All reagents for SDS-PAGE were purchased from BioRad. SDS-PAGE analysis was carried out using 12% (29:1 Acrylamide:Bisacrylamide) gels and visualized with Coomassie Brilliant Blue. DNA sequencing was carried out by the OHSU core facility in the Department of Molecular Microbiology and Immunology. The substrate $preQ_0$ was synthesized as described previously (57) and purified by reverse phase HPLC and stored at room temperature in DMSO. The recombinant aTGT (50) and ArcS (32) from *M. jannaschii* were over-overproduced and purified as previously described. An expression plasmid of a His_6-tagged construct of the Δ172-73 mutant of T7 RNA polymerase (58) was provided by Dr. John Perona.

Instrumentation

Analytical HPLC was performed on an Agilent 1100 series HPLC (G1312A binary pump, G1315A diode array detector). Preparative scale separation was achieved using a Hitachi HPLC (L-

6200 pump and L-4000 single wavelength detector). UV-Vis spectroscopy was carried out on a Varian Cary 100 Bio spectrophotometer fitted with a thermostat-controlled multi-cell holder.

T. kodakarensis strain construction

T. kodakarensis strains markerlessly deleted for TGTa and ArcS = were constructed essentially as described (59) using TS559 as the parental strain. Briefly, non-replicative plasmids were temporarily integrated into the TS559 genome adjacent to the target locus, then excised through homologous recombination between direct repeats flanking the target gene. Markerless deletion of *tgtA* and the non-overlapping sequences of *arcS* were confirmed by diagnostic PCRs using purified genomic DNA as templates (Figure 2, panels B and E, respectively). The exact endpoints of the deletions were confirmed by sequencing amplicons generated from each locus generated with primers that bind to locations adjacent to each locus (primers A and B for *tgtA*; primers E and H for *arcS*). To confirm that neither *tgtA* nor *arcS* was relocated within the *T. kodakarensis* genome, total genomic DNA was purified, digested with either BstEII or BspHI, resolved and transferred for Southern blotting as previously described (60). Two Southern blots probes were employed to confirm the deletion of *tgtA* (probes 1 and 2), and two additional probes (probes 3 and 4) were used to confirm the deletion of *arcS*. Probe 1 was complementary to sequences within *TK0759* that were located on the same BspH1 fragment as *tgtA*, while Probe 2 was complementary to *tgtA* sequences. Probe 3 was complementary to sequences within *TK2152* and *TK2153* that were located on the same BstEII fragment as *arcS*, while Probe 4 was complementary to *arcS* sequences. Information on the construction of probes 1-4 is given below.

Probe #1 was generated with the following primer pair:
Name: S.B. 760extF
Sequence: 5'-AGCAAGGGCGTGAACATCGAGTGGG-3'
Name: S.B. 760extR
Sequence: 5'-GCCCTCTTCAAGGATTCTCTGCACG-3'

Probe #2 was generated with the following primer pair:
Name: S.B. 760intF
Sequence: 5'-AAGGTAGCGAGGTGCTTGCCCTTGG-3'
Name: S.B. 760intR
Sequence: 5'-TGAAACCATCAGCCACCCGATCTTC-3'

Probe #3 was generated with the following primer pair:
Name: 001-2153
Sequence = 5'-CACCTTGAGGATATTAGTGATTGGC-3'
Name: 002-2151
Sequence = 5'-CGTCTATTGAATACTGAGGTTTTCC-3'

Probe #4 was generated with the following primer pair:
Name: S.B. 2156intF
Sequence: 5'-TAGCGATAAGTCCTGTCCTCCTTTG-3'
Name: 002-2155
Sequence: 5'-GGCCAAGTATGACATAGTAGTCACC-3'

Growth of _Thermococcus kodakarensis_ for tRNA isolation

Media preparation: Growth media contained (per liter) yeast extract (2.5 g), tryptone (2.5 g), NaCl (10.2 g), $MgCl_2.6H_2O$ (2.4 g), $MgSO_4$ (0.8 g), $CaCl_2.2H_2O$ (0.4 g), KCl (0.3 g), sodium pyruvate

(2.5 g), agmatine sulfate (0.6 g), 2 mL of a 500x vitamin stock solution (8 µM biotin, 5 µM folic acid, 50 µM pyridoxine, 15 µM thiamine, 15 µM riboflavin, 40 µM nicotinic acid, 20 µM Ca-pantothenate, 7 µM p-aminobenzoic acid and 75 nM B_{12}) and 2 mL of a 500x trace mineral stock solution (50 µM $FeCl_3$, 5 µM $MnCl_2$, 18.5 µM $CoCl_2$, 7 µM $CaCl_2$, 7.5 µM $ZnCl_2$, 1.5 µM $CuCl_2$, 1.6 µM H_3BO_3, 1 µM $(NH_4)_2MoO_4$, 5 µM $NiCl_2$, 850 nM $NaSeO_4$, 2 µM $AlCl_3$). The media was prepared under N_2 to remove all dissolved O_2 (resazurin added to 1 mg/L) and autoclaved to sterilize. Before inoculation the head gas was exchanged for 80:20 N_2/CO_2 to 10 psi. To ensure fully anaerobic conditions, the growth media was spiked with additional Na_2S (from a 2.5% w/v stock) until resazurin remained colorless.

Cell growth: Starter cultures of *T. kodakarensis* [TS559 (wild-type), *ΔTK0760* (*ΔtgtA*) and *ΔTK1256* (*ΔarcS*)] were grown at 60°C overnight in 10 mL cultures in Huntgate tubes with a 1 mL inoculation from stock culture. The cells were then grown in 1 L culture volumes. The media and starter culture were brought to target growth temperature before the entire starter culture was transferred to the larger flask and cells allowed to grow for at least 16 hours. The cells were then pelleted by centrifugation and frozen at -80 ˚C until used.

Comparative growth profiles of *T. kodakarensis* strains

T. kodakarensis strains TS559, Δ*TK0760* and Δ*TK2156* were grown in sealed, 15 mL anaerobic tubes containing 10 mL ASW-YT media (0.8x artificial seawater (ASW), 5g/L yeast extract and 5g/L tryptone) with a headspace gas composition of 95% N_2/5% H_2 at one atmosphere of pressure. Media was supplemented with vitamins and agmatine (as above), and either with 5 g/L pyruvate (- Sulfur), or 2 g/L flowers of sulfur (+ Sulfur). Starter cultures were grown at 85 ˚C, and the optical densities of cultures were monitored at 600 nm during subsequent growth at 70˚, 85˚, and 95˚C, respectively. The results reported are the average values of minimally three independent experiments with triplicate biological replicates in each experiment.

Construction of *M. mazei tgtA* (*MM1101*) insertion mutants

Methanosarcina mazei (DSM no. 3647) gene *MM1101* (*tgtA*) encoding tRNA-guanine transglycosylase (aTGT) was disrupted by insertion of a puromycin resistance cassette in a manner similar to the disruption of the *glnK* gene (48). Briefly, ~1000 bp flanking the 5'- and 3'-regions (Figure 3A) of *tgtA* were amplified from *M. mazei* genomic DNA. The primers for the 5'-flanking region, MM1101ko5primeF: AAAAAA*GGTACC*aaagcaatccataagtgaagc (*Kpn*I) and MM1101ko5primeRL: AAAAA*GAATTC*gccgcggttatagatgc (*EcoR*I) (sequences in the *M. mazei* genome in lower case, restriction sites italicized) introduced *KpnI* and *EcoRI* restriction endonuclease cutting sites at the end of the primers, while the primers for the 3'-flanking region, Mm1101ko3primeF: AAAAA*GAattc*ggaccttcccg (*EcoR*I) and Mm1101ko3primeR: ttca*ggatcc*ctgccg (*BamH*I) (sequences in the *M. mazei* genome in lower case, restriction sites italicized) introduced an *EcoR*I site (a naturally occurring *BamH*I site was used for the reverse primer). Both PCR products were gel purified and introduced into pBluescript by cutting the plasmid and PCR products with *Eco*RI, *Kpn*I and *BamH*I, followed by ligation. The resulting plasmid, pKMSK1, was cut with *EcoR*I and ligated to EcoRI-cut puromycin-resistance cassette (*pac* cassette) (48), generating plasmid pKMSK2. Plasmid constructs were verified by DNA sequencing across ligation junctions. Plasmid pKMSK2 was cut with ScaI to

generate a linear DNA with the *pac* cassette with ca. 1000 bp of sequence flanking *MM1101*. This DNA was transformed into *M. mazei* with DOTAP liposome-mediated transformation (48). Transformants were grown in the presence of puromycin three independent isolates, *M. mazei* *ΔtgtA1*, *ΔtgtA2*, *ΔtgtA3* were selected as single clones on plates containing puromycin. Insertion mutations were confirmed by PCR (Figure 3B), with mutants containing the *pac* gene and lacking the *tgtA* gene and Southern Blots using flanking probes or *pac* probes. The flanking probe was made by PCR using primers (Mma_attP_5'Flank): 5'-GGCTTACTCCCGCTTTCTCT-3' and (Mma_attP_3'Flank): 5'-TTGAGTTCCTCGCTTTCGAT-3' and DIG nucleotide mix (Roche). The *pac* probe was made by PCR using (KMSPacR (Mm1101_5'R_rc) 5'-GCATCTATAACCGCGGC-3' and KMSPacF (Mm1101_3'F_rc) 5'-CGGGAAGGTCCCGAAT-3' and DIG nucleotide mix (Roche).

Growth of *M. mazei* and mutants

For growth at different temperatures *M. mazei* cells were grown essentially as described (48). Cells were grown anaerobically in closed 5 mL culture tubes with 25 mM trimethylamine reduced with 2 mM cysteine and 1 mM sodium sulfide and an overpressure of N_2/CO_2. Cultures were supplemented with 100 μg/mL ampicillin or 100 μg/mL kanamycin to prevent bacterial growth. Mutants were selected with 2.5 μg/mL puromycin. Growth was monitored by measuring the optical density at 600 nm. For screening for growth changes of mutant strains under different conditions a microtiter plate assay modified for growth in anaerobic conditions was used (61). Reduction was performed only with cysteine and not with sodium sulfide. Growth was monitored until stationary phase was reached.

tRNA extraction from *T. kodakarensis* and *M. mazei*

T. kodakarensis or *M. mazei* cells were suspended at 250 mg/mL in 100 mM ammonium acetate (pH 6.5) with 10 mM $MgSO_4$ and 0.1 mM EDTA. An equal volume of saturated phenol mix (phenol:choloroform:isoamyl alcohol (25:24:1)) was added to lyse the cells, and after centrifugation to separate the phases the bulk RNA was precipitated from the aqueous phase by adding $1/10^{th}$ volume of 8.0 M ammonium acetate and two volumes of ethanol and cooling to -20 °C for two hours. The precipitated RNA was pelleted by centrifugation at 20,000*xg* for 25 minutes at 4 °C. The pellet was resuspended in 100 mM ammonium acetate (pH 6.5) with 10 mM $MgSO_4$ and 0.1 mM EDTA, an equal volume of 8.0 M LiCl was added, and the mix cooled at 4 °C overnight. Precipitated rRNA species were removed by centrifugation (20,000*xg*), followed by precipitation of the tRNA remaining in the supernatant with the addition of ammonium acetate/ethanol as above.

To determine the modification state of the tRNA from each strain the purified unfractionated tRNA samples were enzymatically digested and dephosphorylated as described preciously (62), followed by HPLC analysis on large (250 x 4.6 mm) or small (30 x 4.6 mm) Gemini columns (Phenomenex, 5 μm C18). The mobile phase consisted of a variable gradient from 100% 25 mM ammonium acetate (pH 6.0) (solvent A) to a 60:40 mix of solvent A and solvent B (acetonitrile) over the course of 20-25 minutes.

Isolation of tRNA from *T. kodakarensis* for mass spectrometric analysis

Total RNA was extracted as above, however to prepare total tRNA for MS analysis solid phase extraction was employed to reduce the counter ion species present. Nucleobond RNA/DNA 400 columns (Macherey-Nagel) were employed to separate high mass RNA molecules and total tRNA. Pelleted total tRNA was suspended in the appropriate buffer according to the manufacturer's guidelines, and fractionation utilized a step gradient of salt concentration with tRNA eluting in 0.65 M KCl and higher mass molecules eluting in 1.15M KCl. The RNA population in sub-fractions were confirmed by urea PAGE. The isolated tRNA was precipitated in 800 mM ammonium acetate/ethanol. This was repeated three times to substitute the K^+ with ammonium ions. The sample was then dried for subsequent LCMS analysis.

The purified unfractionated tRNA samples were enzymatically digested and dephosphorylated as described preciously (62). Separation was accomplished by reversed phase chromatography using an Acquity UPLC HSS T3 column (1.8 µm, 1 mm X 100 mm; Waters, Milford, MA) on a Vanquish Flex Quaternary UHPLC system (Thermo Fisher Scientific, San Jose, CA). The mobile phase A consisted of 5.3 mM ammonium acetate (pH 5.3) in LC-MS grade water (Alfa Aesar, Haverhill, MA). Mobile phase B consisted of a 60:40 mixture of 5.3 mM ammonium acetate (pH 5.3) and acetonitrile (Honeywell Burdick & Jackson, Morris Plains, NJ) with a gradient of 0% B (from 0 to 1.8 min), 2% B at 3 to 3.5 min, 3% B at 4.1 min, 5% B at 7 min, 25% B at 9 min, 35% B at 15 min, 99% B at 15.5 min (hold for 4.5 min), 99% B at 20 min then returning to 0% B at 25.5 min at a flow rate of 100 µL min^{-1}. The column temperature was set at 40 °C.

High-resolution accurate mass analyses of nucleosides were performed on an Orbitrap Fusion Lumos Tribrid mass spectrometer (Thermo Fisher Scientific) interfaced with an H-ESI electrospray source in positive polarity mode. Full scan data was acquired at a resolution of 120,000, mass range 220-900 *m/z*, AGC 7.5e4, and IT 100 ms. Data-dependent top speed MS/MS spectra (1 s cycle, CID 42%) were acquired in the ion trap at a resolution of 15,000, AGC 1.0e4, and IT 150 ms. The other instrumental conditions were the following: quadrupole isolation of 1 *m/z*; RF 35%; sheath gas, auxiliary gas, and sweep gas of 30, 10 and 0 arbitrary units, respectively; ion transfer tube temperature of 289 °C; vaporizer temperature of 92 °C; and spray voltage of 3500 V. Data was analyzed using Xcalibur 4.0, Compound Discoverer 3.0 and MzVault 2.1 (Thermo Fisher Scientific).

Isolation of isoacceptor tRNA from *T. kodakarensis*

To purify $tRNA^{Gln}$ from the *T. kodakarensis* strains we opted to employ an affinity approach based on hybridization with a DNA oligo complementary to a portion of the target tRNA (49). The area most distinct for Gln sequences among all *T. kodakarensis* tRNA sequences is from the ASL leading to the 3' end of the molecule. However, since both isoacceptors for the Gln encoding tRNA are identical except for a single position in the anticodon, it was not possible to isolate the CUG or UUG isoacceptor free of the other. Nevertheless, we reasoned that a single nucleotide difference in the sequence of the ACL should be of no consequence to the overall stability of the tRNA, so the isolation of a mixture containing both isoacceptors would not compromise the experiment.

Potential DNA affinity oligos were designed by walking along the length of the tRNA in 3 nt steps beginning at position 26 (Supplemental Figure 6A). By first investigating the ability of each oligo

to hybridize with an *in vitro* synthesized $tRNA^{Gln}$ transcript corresponding to *T. kodakarensis* $tRNA^{Gln}$(CUG) via native PAGE we identified Aff3 as the best candidate for forming a stable hybrid with the *in vivo* $tRNA^{Gln}$ from *T. kodakarensis* (Supplemental Figure 6B).

The streptavidin agarose (Thermo Scientific) resin was activated by binding the Aff3 biotinylated oligo to the streptavidin (oligo at 15 µM in 10 mM Tris-HCl (7.5), 100 mM NaCl). For annealing of the tRNA to the immobilized DNA, the total tRNA was dissolved in annealing buffer (10 mM Tris-HCl (7.5), 900 mM NaCl, 1mM EDTA) and heated to 95°C for 5 minutes. After cooling to 85°C the resin (pre-equilibrated in annealing buffer) was added and the slurry allowed to fully cool to room temperature with occasional mixing. The resin was pelleted by centrifugation (5,000*xg*) and the unbound RNA was removed with the supernatant. Annealing buffer was added to wash the resin followed by heating to 45 ˚C for 5 minutes to remove non-specifically bound tRNA, centrifugation, and removal of the supernatant. This process was repeated until the OD260 of the supernatant was below 0.01 AU/mL. Elution of the $tRNA^{Gln}$ was achieved by re-suspending the resin in 0.5 mL of elution buffer (10 mM Tris-HCl (7.5), 100 mM NaCl), heating the solution to 75 °C for 5 minutes, and centrifuging to collect the unbound $tRNA^{Gln}$ (Supplemental Figure 7). The isolated tRNA was shown to be homogenous in both denaturing (Urea TBE) and native (TB, 100 mM NaCl) PAGE (Supplemental Figure 8).

Production of tRNA transcripts *in vitro*

Double stranded template DNA was designed based on the sequence of $tRNA^{Gln}$(CUG) from *T. kodakarensis* (below), with the exception that the native gene sequence was modified by changing the 5' adenosine nucleotide to a guanosine (double underline) for enhanced transcription yield (63).

5'GGCCCCGUGGUGUAGCGGCCAAGCAUGCGGGACUCUGGAUCCCGCGACCGGGGUUCGAAUCCCCGCG
GGGCUACCA3'

The template DNA was prepared from two DNA oligos (below) that were designed with a ten base pair overlap at the center of the target sequence (underlined), and which contained 2'-O-methyl modifications on the two terminal 5-residues of the template strand (63) and the standard T7 promoter at the 5' end of the non-template strand (bold).

5'**TAATACGACTCACTATA**GGCCCCGTGGTGTAGCGGCCAAGCATGCGGGA3'
5'mUmGGTAGCCCCGCGGGGATTCGAACCCCGGTCGCGGGATCCAGAGTCCCGCATGC3

The complete template was generated by primer extension using the Klenow fragment (Fermentas) to create two fully complementary strands. The two oligos were mixed to a final concentration of 4 µM each, in the presence of dNTPs (600 µM each) and using the manufacturers reaction conditions. The primers were extended by cycling 25 times between 37 °C and 10 °C in 30 second pulses (Applied Biosystems 2720 thermal cycler). The DNA was then isolated by organic extraction (equal volume of 25:24:1 phenol:chloroform:isoamyl alcohol vortexed and then centrifuged at 20,000*g* for 5 minutes) and ethanol precipitation of the aqueous phase. The template was then resuspended in water at 10 µM.

RNA was transcribed from 1 µM DNA template in 30 mM Tris-HCl (pH 8.0), 40 mM $MgCl_2$, 10 mM DTT, 0.1% Triton X-100, 100 µM spermidine, 2.5 mM NTP (individual nucleotides obtained from Sigma, stock made up in DEPC water and stored at -80 °C), 50 µg/mL of the Δ172-73 mutant of T7 RNA polymerase (58) and 1 U/mL of inorganic pyrophosphatase (Sigma). The reactions were run for 4 hrs at 37 °C and quenched by ethanol precipitation. The recovered pellet was solubilized in DEPC water and then mixed with an equal volume of formamide/5 mM EDTA. The reaction products were denatured at 95°C and then separated by denaturing urea PAGE (7 M urea, 10% acrylamide, 1x TBE, gel run at 18W). The full-length product band was excised from the gel and the RNA extracted by overnight crush and soak in 800 mM ammonium acetate. The purified RNA was then precipitated with the addition of ethanol and the pellet resuspended in 1.0 mM sodium citrate (pH 6.3) and stored at -80°C.

Preparation of $preQ_0$ and G^+ modified tRNA

The $tRNA^{Gln}$(CUG) transcript was modified by incorporation of $preQ_0$ base at position 15 by the action of *M. jannaschii* aTGT. The activity of the enzyme was determined by substituting [8-^{14}C]-guanine in place of $preQ_0$ in a standard reaction assay (50), which established the conditions for quantitative incorporation of $preQ_0$. Reaction conditions were 50 mM succinate (pH 5.5), 20 mM $MgCl_2$, 100 mM KCl, 2 mM DTT, 100 µM tRNA and 1 mM $preQ_0$. The reaction solution containing tRNA was heated at 80°C for 3 minutes before the addition of aTGT to a final concentration of 10 µM and incubation at 80 ˚C for 1 hour. The reaction was repeated for two more rounds of incorporation to ensure complete substitution with $preQ_0$ base. The reaction was terminated by the addition of 1/10th volume of 8M ammonium acetate. Reaction components were removed by phenol/chloroform extraction, and the tRNA isolated by ethanol precipitation of the aqueous phase. The tRNA pellet was resuspended in 1.0 mM sodium citrate (pH 6.3) and stored at -80°C.

To produce G^+-modified tRNA a sample of $preQ_0$-modified tRNA was suspended (50 µM) in 100 mM HEPES (pH 7.0), 0.5 M NaCl, 20 mM $MgCl_2$, 5.0 mM glutamine, 1.0 mM DTT and 10 µM *M. jannaschii* ArcS. The sample was reacted for 1 hour at 40°C. The modified RNA was isolated as described above. Samples of both $preQ_0$- and G^+-modified tRNA were digested, dephosphorylated, and analyzed by HPLC as described above to confirm the modification status (Supplementary Figure 5).

UV thermal denaturation studies

All thermal denaturation studies were performed on a Cary 100 Bio UV-Vis spectrophotometer. Single wavelength absorbance at 260 nm was used to record the unfolding of the tRNA species being studied. Temperature was maintained by a thermostat-controlled cell block holder. The thermal melt cycle was controlled by the Thermal program in the Cary Win UV software suite. Samples were prepared in 10 mM sodium cacodylate (pH 7.0) and 100 mM NaCl. This was supplemented with either EDTA or $MgCl_2$ for experiments lacking or containing $MgCl_2$, respectively. RNA was heated in buffer to 98 ˚C and slow cooled to 55°C, at which point EDTA or $MgCl_2$ was added and the sample allowed to cool to room temperature. During analysis, the sample volume (120µL) was covered with mineral oil to prevent evaporation. The raw absorbance vs temperature

data was converted to a differential profile ($dAbs_{260}/dT$ vs temperature) and the T_m determined from these plots.

ACKNOWLEDGEMENT

The Iwata-Reuyl lab acknowledges Professor David Draper for engaging discussions about Mg^{2+}-RNA binding. This work was supported with funding from NASA (NNX07AJ26G to D.I.-R. and K.S.), the Alexander von Humboldt Foundation (to K.S. and R.S.), and the Department of Energy, Basic Energy Sciences Division (DE-SC0014597 to T.J.S.)

CONFLICT OF INTEREST

The authors declare no conflicts of interest.

REFERENCES

1. Bjork, G.R. (1995) In Soll, D. and RajBhandary, U. L. (eds.), *tRNA: Structure, Biosynthesis, and Function*. ASM Press, Washington D. C., pp. 165-206.
2. Cantara, W.A., Crain, P.F., Rozenski, J., McCloskey, J.A., Harris, K.A., Zhang, X., Vendeix, F.A., Fabris, D. and Agris, P.F. (2011) The RNA Modification Database, RNAMDB: 2011 update. *Nucleic Acids Res*, **39**, D195-201.
3. Boccaletto, P., Machnicka, M.A., Purta, E., Piatkowski, P., Baginski, B., Wirecki, T.K., de Crecy-Lagard, V., Ross, R., Limbach, P.A., Kotter, A. *et al.* (2018) MODOMICS: a database of RNA modification pathways. 2017 update. *Nucleic Acids Res*, **46**, D303-D307.
4. Yokoyama, S. and Nishimura, S. (1995) In Soll, D. and RajBhandary, U. L. (eds.), *tRNA: Structure, Biosynthesis, and Function*. ASM Press, Washington D. C.
5. Bjork, G.R. (1992) In Hatfield, D. L., Lee, B. L. and Pirtle, R. M. (eds.), *Transfer RNA in Protein Synthesis*. CRC Press, Inc., Boca Raton, pp. 23-85.
6. Muramatsu, T., Nishikawa, K., Nemoto, F., Kuchino, Y., Nishimura, S., Miyazawa, T. and Yokoyama, S. (1988) Codon and Amino-Acid Specificities of a Transfer RNA are Both Converted by a Single Post-Transcriptional Modification. *Nature*, **336**, 179-181.
7. Muramatsu, T., Yokoyama, S., Horie, N., Matsuda, A., Ueda, T., Yamaizumi, Z., Kuchino, Y., Nishimura, S. and Miyazawa, T. (1988) A Novel Lysine-Substituted Nucleoside in the First Position of the Anti-Codon of Minor Isoleucine tRNA From *Escherichia coli*. *J Biol Chem*, **263**, 9261-9267.
8. Thiaville, P.C., Legendre, R., Rojas-Benitez, D., Baudin-Baillieu, A., Hatin, I., Chalancon, G., Glavic, A., Namy, O. and de Crecy-Lagard, V. (2016) Global translational impacts of the loss of the tRNA modification t6A in yeast. *Microb Cell*, **3**, 29-45.
9. Kowalak, J.A., Dalluge, J.J., McCloskey, J.A. and Stetter, K.O. (1994) The role of posttranscriptional modification in stabilization of transfer RNA from hyperthermophiles. *Biochemistry*, **33**, 7869-7876.
10. Derrick, W.B. and Horowitz, J. (1993) Probing structural differences between native and in vitro transcribed Escherichia coli valine transfer RNA: evidence for stable base modification-dependent conformers. *Nucleic Acids Res*, **21**, 4948-4953.
11. Perret, V., Garcia, A., Puglisi, J., Grosjean, H., Ebel, J.P., Florentz, C. and Giege, R. (1990) Conformation in solution of yeast tRNA(Asp) transcripts deprived of modified nucleotides. *Biochimie*, **72**, 735-743.

12. Horie, N., Hara-Yokoyama, M., Yokoyama, S., Watanabe, K., Kuchino, Y., Nishimura, S. and Miyazawa, T. (1985) Two tRNAIle1 species from an extreme thermophile, Thermus thermophilus HB8: effect of 2-thiolation of ribothymidine on the thermostability of tRNA. *Biochemistry*, **24**, 5711-5715.
13. Lorenz, C., Lunse, C.E. and Morl, M. (2017) tRNA Modifications: Impact on Structure and Thermal Adaptation. *Biomolecules*, **7**(2). E35.
14. Persson, B.C. (1993) Modification of tRNA as a regulatory device. *Mol. Microbiol.*, **8**, 1011-1016.
15. Li, S., Xu, Z. and Sheng, J. (2018) tRNA-Derived Small RNA: A Novel Regulatory Small Non-Coding RNA. *Genes*, **9**(5), 246.
16. Geslain, R. and Pan, T. (2011) tRNA: Vast reservoir of RNA molecules with unexpected regulatory function. *Proc Natl Acad Sci USA*, **108**, 16489-16490.
17. Gregson, J.M., Crain, P.F., Edmonds, C.G., Gupta, R., Hashizume, T., Phillipson, D.W. and McCloskey, J.A. (1993) Structure of Archaeal Transfer RNA Nucleoside G*-15 (2-Amino-4,7-dihydro-4-oxo-7-b-D-ribofuranosyl-1*H*-pyrrolo[2,3-*d*]pyrimidine-5-carboximidamide (Archaeosine)). *J Biol Chem*, **268**, 10076-10086.
18. Kasai, H., Ohashi, Z., Harada, F., Nishimura, S., Oppenheimer, N.J., Crain, P.F., Liehr, J.G., von Minden, D.L. and McCloskey, J.A. (1975) Structure of the Modified Nucleoside Q Isolated from *Escherichia coli* Transfer Ribonucleic Acid. 7-(4,5-*cis*-Dihydroxy-1-cyclopenten-3-ylaminomethyl)-7-deazaguanosine. *Biochemistry*, **14**, 4198-4208.
19. Katz, J.R., Basile, B. and McCloskey, J.A. (1982) Queuine, a Modified Base Incorporated Posttranscriptionally into Eukaryotic Transfer RNA: Wide Distribution in Nature. *Science*, **216**, 55-56.
20. Kersten, H. (1988) The Nutrient Factor Queuine: Biosynthesis, Occurence in Transfer RNA and Function. *BioFactors*, **1**, 27-29.
21. Sprinzl, M., Hartmann, T., Weber, J., Blank, J. and Zeidler, R. (1989) Compilation of tRNA Sequences and Sequences of tRNA Genes. *Nucleic Acids Res*, **17**, r1-r67.
22. Kawamura, T., Hirata, A., Ohno, S., Nomura, Y., Nagano, T., Nameki, N., Yokogawa, T. and Hori, H. (2016) Multisite-specific archaeosine tRNA-guanine transglycosylase (ArcTGT) from Thermoplasma acidophilum, a thermo-acidophilic archaeon. *Nucleic Acids Res*, **44**, 1894-1908.
23. Iwata-Reuyl, D. and de Crécy Lagard, V. (2009) In Grosjean, H. (ed.), *DNA and RNA Modification Enzymes: Structure, Mechanism, Function and Evolution*. Landes Bioscience, New York, pp. 379-394.
24. Phillips, G., El Yacoubi, B., Lyons, B., Alvarez, S., Iwata-Reuyl, D. and de Crecy-Lagard, V. (2008) Biosynthesis of 7-deazaguanosine-modified tRNA nucleosides: a new role for GTP cyclohydrolase I. *J Bacteriol*, **190**, 7876-7884.
25. Sankaran, B., Bonnett, S.A., Shah, K., Gabriel, S., Reddy, R., Schimmel, P., Rodionov, D.A., de Crecy-Lagard, V., Helmann, J.D., Iwata-Reuyl, D. Swairjo, M.A. (2009) Zinc-independent folate biosynthesis: genetic, biochemical, and structural investigations reveal new metal dependence for GTP cyclohydrolase IB. *J Bacteriol*, **191**, 6936-6949.
26. El Yacoubi, B., Bonnett, S., Anderson, J.N., Swairjo, M.A., Iwata-Reuyl, D. and de Crecy-Lagard, V. (2006) Discovery of a new prokaryotic type I GTP cyclohydrolase family. *The J Biol Chem*, **281**, 37586-37593.
27. Grochowski, L.L., Xu, H., Leung, K. and White, R.H. (2007) Characterization of an Fe(2+)-dependent archaeal-specific GTP cyclohydrolase, MptA, from Methanocaldococcus jannaschii. *Biochemistry*, **46**, 6658-6667.
28. Mashhadi, Z., Xu, H. and White, R.H. (2009) An Fe2+-dependent cyclic phosphodiesterase catalyzes the hydrolysis of 7,8-dihydro-D-neopterin 2',3'-cyclic phosphate in methanopterin biosynthesis. *Biochemistry*, **48**, 9384-9392.

29. McCarty, R.M., Somogyi, A. and Bandarian, V. (2009) Escherichia coli QueD Is a 6-Carboxy-5,6,7,8-tetrahydropterin Synthase (dagger). *Biochemistry*, **48**, 2301 - 2303.
30. Dowling, D.P., Bruender, N.A., Young, A.P., McCarty, R.M., Bandarian, V. and Drennan, C.L. (2014) Radical SAM enzyme QueE defines a new minimal core fold and metal-dependent mechanism. *Nat Chem Biol*, **10**, 106-112.
31. Nelp, M.T. and Bandarian, V. (2015) A Single Enzyme Transforms a Carboxylic Acid into a Nitrile through an Amide Intermediate. *Angew Chem Int Ed Engl*, **54**, 10627-10629.
32. Phillips, G., Chikwana, V.M., Maxwell, A., El-Yacoubi, B., Swairjo, M.A., Iwata-Reuyl, D. and de Crecy-Lagard, V. (2010) Discovery and characterization of an amidinotransferase involved in the modification of archaeal tRNA. *J Biol Chem,* **285**, 12706-12713.
33. Bon Ramos, A., Bao, L., Turner, B., de Crecy-Lagard, V. and Iwata-Reuyl, D. (2017) QueF-Like, a Non-Homologous Archaeosine Synthase from the Crenarchaeota. *Biomolecules*, **7**.
34. Phillips, G., Swairjo, M.A., Gaston, K.W., Bailly, M., Limbach, P.A., Iwata-Reuyl, D. and de Crecy-Lagard, V. (2012) Diversity of archaeosine synthesis in crenarchaeota. *ACS Chem Biol*, **7**, 300-305.
35. Van Lanen, S.G., Reader, J.S., Swairjo, M.A., de Crecy-Lagard, V., Lee, B. and Iwata-Reuyl, D. (2005) From cyclohydrolase to oxidoreductase: discovery of nitrile reductase activity in a common fold. *Proc Natl Acad Sci USA*, **102**, 4264-4269.
36. Kinzie, S.D., Thern, B. and Iwata-Reuyl, D. (2000) Mechanistic studies of the tRNA-modifying enzyme QueA: a chemical imperative for the use of AdoMet as a "ribosyl" donor. *Organic Lett*, **2**, 1307-1310.
37. Miles, Z.D., McCarty, R.M., Molnar, G. and Bandarian, V. (2011) Discovery of epoxyqueuosine (oQ) reductase reveals parallels between halorespiration and tRNA modification. *Proc Natl Acad Sci USA*, **108**, 7368-7372.
38. Zallot, R., Ross, R., Chen, W.H., Bruner, S.D., Limbach, P.A. and De Crecy-Lagard, V. (2017) Identification of a novel epoxyqueuosine reductase family by comparative genomics. *ACS Chem Biol*. **12**(3), 844-851.
39. Boland, C., Hayes, P., Santa-Maria, I., Nishimura, S. and Kelly, V.P. (2009) Queuosine formation in eukaryotic tRNA occurs via a mitochondria-localized heteromeric transglycosylase. *J Biol Chem*, **284**, 18218-18227.
40. Kersten, H. and Kersten, W. (1990) In Gehrke, C. W. and Kuo, K. C. T. (eds.), *Chromatography and Modification of Nucleosides Part B*. Elsevier, Amsterdam, pp. B69-B108.
41. Marks, T. and Farkas, W.R. (1997) Effects of a diet deficient in tyrosine and queuine on germfree mice. *Biochem Biophys Res Commun*, **230**, 233-237.
42. Carlson, B.A., Kwon, S.Y., Chamorro, M., Oroszlan, S., Hatfield, D.L. and Lee, B.J. (1999) Transfer RNA modification status influences retroviral ribosomal frameshifting. *Virology*, **255**, 2-8.
43. Durand, J., Okada, N., Tobe, T., Watarai, M., Fukuda, I., Suzuki, T., Nakata, N., Komatsu, K., Yoshikawa, M. and Sasakawa, C. (1994) *vacC*, a Virulence-Associated Chromosomal Locus of *Shigella flexneri*, is Homologous to *tgt*, a Gene Encoding tRNA-Guanine Transglycosylase (Tgt) of *E. coli* K-12. *J Bacteriol*, **176**, 4627-4634.
44. Rakovich, T., Boland, C., Bernstein, I., Chikwana, V.M., Iwata-Reuyl, D. and Kelly, V.P. (2011) Queuosine deficiency in eukaryotes compromises tyrosine production through increased tetrahydrobiopterin oxidation. *J Biol Chem*, **286**, 19354-19363.
45. Oliva, R., Tramontano, A. and Cavallo, L. (2007) Mg2+ binding and archaeosine modification stabilize the G15 C48 Levitt base pair in tRNAs. *RNA*, **13**, 1427-1436.
46. Orita, I., Futatsuishi, R., Adachi, K., Ohira, T., Kaneko, A., Minowa, K., Suzuki, M., Tamura, T., Nakamura, S., Imanaka, T. *et al.* (2019) Random mutagenesis of a hyperthermophilic archaeon identified tRNA modifications associated with cellular hyperthermotolerance. *Nucleic Acids Res*, **47**, 1964-1976.

47. Deppenmeier, U., Johann, A., Hartsch, T., Merkl, R., Schmitz, R.A., Martinez-Arias, R., Henne, A., Wiezer, A., Baumer, S., Jacobi, C. *et al.* (2002) The genome of *Methanosarcina mazei*: evidence for lateral gene transfer between bacteria and archaea. *J Mol Microbiol Biotechnol*, **4**, 453-461.
48. Ehlers, C., Weidenbach, K., Veit, K., Deppenmeier, U., Metcalf, W.W. and Schmitz, R.A. (2005) Development of genetic methods and construction of a chromosomal *glnK*$_1$ mutant in *Methanosarcina mazei* strain Goe1. *Mol Genet Genomics*, **273**, 290-298.
49. Kazayama, A., Yamagami, R., Yokogawa, T. and Hori, H. (2015) Improved solid-phase DNA probe method for tRNA purification: large-scale preparation and alteration of DNA fixation. *J Biochem*, **157**, 411-418.
50. Bai, Y., Fox, D.T., Lacy, J.A., Van Lanen, S.G. and Iwata-Reuyl, D. (2000) Hypermodification of tRNA in Thermophilic archaea. Cloning, overexpression, and characterization of tRNA-guanine transglycosylase from Methanococcus jannaschii. *J Biol Chem*, **275**, 28731-28738.
51. Thiaville, J.J., Kellner, S.M., Yuan, Y., Hutinet, G., Thiaville, P.C., Jumpathong, W., Mohapatra, S., Brochier-Armanet, C., Letarov, A.V., Hillebrand, R. *et al.* (2016) Novel genomic island modifies DNA with 7-deazaguanine derivatives. *Proc Natl Acad Sci USA*, **113**, E1452-1459.
52. Blaby, I.K., Phillips, G., Blaby-Haas, C.E., Gulig, K.S., El Yacoubi, B. and de Crecy-Lagard, V. (2010) Towards a systems approach in the genetic analysis of archaea: Accelerating mutant construction and phenotypic analysis in Haloferax volcanii. *Archaea*, **2010**, 426239.
53. Davanloo, P., Sprinzl, M., Watanabe, K., Albani, M. and Kersten, H. (1979) Role of ribothymidine in the thermal stability of transfer RNA as monitored by proton magnetic resonance. *Nucleic Acids Research*, **6,** 1571-1581.
54. Nomura, Y., Ohno, S., Nishikawa, K. and Yokogawa, T. (2016) Correlation between the stability of tRNA tertiary structure and the catalytic efficiency of a tRNA-modifying enzyme, archaeal tRNA-guanine transglycosylase. *Genes Cells*, **21**, 41-52.
55. Watanabe, M., Nameki, N., Matsuo-Takasaki, M., Nishimura, S. and Okada, N. (2001) tRNA recognition of tRNA-guanine transglycosylase from a hyperthermophilic archaeon, Pyrococcus horikoshii. *J Biol Chem*, **276**, 2387-2394.
56. Wolf, B., Lesnaw, J.A. and Reichmann, M.E. (1970) A mechanism of the irreversible inactivation of bovine pancreatic ribonuclease by diethylpyrocarbonate. A general reaction of diethylpyrocarbonate . A general reaction of diethylpyrocarbonate with proteins. *Eur J Biochem*, **13**, 519-525.
57. Migawa, M.T., Hinkley, J.M., Hoops, G.C. and Townsend, L.B. (1996) A Two Step Synthesis of the Nucleoside Q Precursor 2-Amino-5-cyanopyrrolo[2,3-*d*]pyrimidin-4-one (PreQ$_0$). *Synth. Comm.*, **26**, 3317-3322.
58. Lyakhov, D.L., He, B., Zhang, X., Studier, F.W., Dunn, J.J. and McAllister, W.T. (1997) Mutant bacteriophage T7 RNA polymerases with altered termination properties. *J Mol Biol*, **269**, 28-40.
59. Hileman, T.H. and Santangelo, T.J. (2012) Genetics Techniques for Thermococcus kodakarensis. *Front Microbiol*, **3**, 195.
60. Santangelo, T.J., Cubonova, L., James, C.L. and Reeve, J.N. (2007) TFB1 or TFB2 is sufficient for Thermococcus kodakaraensis viability and for basal transcription in vitro. *J Mol Biol*, **367**, 344-357.
61. Bang, C., Schilhabel, A., Weidenbach, K., Kopp, A., Goldmann, T., Gutsmann, T. and Schmitz, R.A. (2012) Effects of antimicrobial peptides on methanogenic archaea. *Antimicrob Agents Chemother*, **56**, 4123-4130.
62. Pomerantz, S.C. and McCloskey, J.A. (1990) Analysis of RNA Hydrolyzates by Liquid Chromatography-Mass Spectrometry. *Meth Enzymol*, **193**, 796-824.
63. Sherlin, L.D., Bullock, T.L., Nissan, T.A., Perona, J.J., Lariviere, F.J., Uhlenbeck, O.C. and Scaringe, S.A. (2001) Chemical and enzymatic synthesis of tRNAs for high-throughput crystallization. *RNA*, **7**, 1671-1678.

FIGURE LEGENDS

Figure 1. The biosynthetic pathways to archaeosine (G^+) and queuosine (Q).

Figure 2. *T. kodakarensis* strains markerlessly deleted for TK0760 (7-cyano-7-deazaguanine tRNA-ribosyltransferase) and TK2156 (archaeosine synthase). **Panels A & B.** Map of the *T. kodakarensis* genome surrounding TK0760 (panel A) and TK2156 (panel D) in the parental strain TS559 highlighting the binding positions of oligonucleotides that were used in diagnostic PCRs (panel B and E, respectively) and Southern blots (panels C and F, respectively). **Panels B & E**. PCRs with primer sets listed above each lane generate amplicons from genomic DNA purified from strains TS559, ΔTK0760 and ΔTK2156. The external primer pairs (A/B for TK0760; E/H for TK2156) generate smaller amplicons from ΔTK0760 and ΔTK2156 genomic DNAs, respectively, reflecting the loss of TK0760 or TK2156 coding sequences. Amplicons generated using one primer complementary to the target locus and one primer complementary to flanking sequences are only generated from TS559 genomic DNA, consistent with deletion of the TK0760 or TK2156 coding sequences, respectively. M = DNA standards in Kbp. **Panels C & F**. Southern blots of digested total genomic DNA from strains TS559, ΔTK0760 and ΔTK2156 demonstrate deletion of TK0760 or TK2156, respectively. Blots developed with an amplicon complementary to the TK0760 coding sequences (probe 2) reveal a complementary target only from TS559 DNA, while an amplicon probe complementary to adjacent sequences (probe 1) within the same BspH1 fragment reveals a smaller target, consistent with deletion of TK0760 coding sequences. Blots developed with an amplicon complementary to the TK2156 coding sequences (probe 4) reveal a complementary target only from TS559 DNA, while an amplicon probe complementary to adjacent sequences (probe 3) within the same BstEII fragment reveals a smaller target, consistent with deletion of TK2156 coding sequences.

Figure 3. *M. mazei* strains deleted for *MM1101* (7-cyano-7-deazaguanidine tRNA ribosyltransferase). **A.** Map of the *M. mazei* genome surrounding *MM1101* (*tgtA*) in the parental strain *M. mazei* highlighting the binding positions of oligonucleotides that were used in diagnostic PCRs (Panel B) and Southern Blots (Panel C). **B**. PCR with primer sets listed above each lane generate amplicons from genomic DNA purified from wild-type and mutant (*M. mazei ΔtgtA*) strains. Amplicons generated by primers specific for the *tgtA* gene demonstrate the presence of *tgtA* in the wild-type and loss of *tgtA* in *M. mazei ΔtgtA*. By contrast, amplicons generated from the puromycin (*pac*) cassette indicate that it is present in *M. mazei ΔtgtA* and absent in the wild-type strain. **C**. Southern Blots of PstI digested total genomic DNA from wild-type and *M. mazei ΔtgtA* demonstrate loss of *tgtA* in *M. mazei ΔtgtA*. Blots developed with an amplicon complementary to sequences adjacent to *tgtA* (probe 1) reveal a smaller target, consistent with the deletion of *tgtA* and insertion of the *pac* cassette. Blots developed with an amplicon complementary to the *pac* cassette reveal a complementary target only in *M. mazei ΔtgtA*, consistent with a *pac* cassette insertion into the *M. mazei ΔtgtA* strain.

Figure 4. Analysis of modification status of tRNA isolated from *T. kodakarensis* strains. **A.** HPLC analysis of nucleoside digests of tRNA from *T. kodakarensis* TS559 (bottom trace), the *ΔarcS* strain (middle trace), and the *Δtgt* strain (top trace). **B.** LCMS analysis of nucleoside digests of tRNA from *T. kodakarensis* TS559: Extracted ion chromatograms of archaeosine *m/z*: 325.1257 (top) and $preQ_0$-nucleoside *m/z*: 308.0994 (bottom). XICs relative abundances were scaled to largest peak (archaeosine) at 10^6. Signal for $preQ_0$-nucleoside was detected at background levels 10^3. **C.** LCMS analysis of nucleoside digests of tRNA from the *T. kodakarensis Δtgt* strain: Extracted ion chromatograms of archaeosine *m/z*: 325.1257 (top) and $preQ_0$-nucleoside *m/z*: 308.0994 (bottom). Neither archaeosine nor $preQ_0$ were detected at any appreciable levels. Chromatograms scaled 10^3. **D.** LCMS analysis of nucleoside digests of tRNA from the *T. kodakarensis ΔarcS* strain: Extracted ion chromatograms of archaeosine *m/z*: 325.1257 (top) and $preQ_0$-nucleoside *m/z*: 308.0994 (bottom). For this run G^+ was detected at 1.6% that of $preQ_0$-nucleoside. Asterisk denotes the adduction of ammonium onto the $preQ_0$-nucleoside during the electrospray process. Chromatograms scaled 10^6. Analyses were carried out in triplicate for each of two independent preparations of tRNA.

Figure 5. *T. kodakarensis* strains lacking *tgtA* or *arcS* are temperature sensitive. Culture growth was monitored by changes in optical density at 600 nm for cultures incubated at 70˚C (panels A & D), 85˚C (panels B & E), or 95˚C (panels C & F). The results reported are the average values of minimally three independent experiments with triplicate biological replicates in each experiment. Cultures in

809 panels A-C were provided 2 g/l sufur, while cultures in panels D-F received 5 g/l pyruvate instead.
810 Filled, black squares, TS559; filled, dark grey triangles, Δ*tgtA*; filled, light grey circles, Δ*arcS*.

811 **Figure 6**. Thermal denaturation profiles (1st derivative) of *in vivo T. kodakarensis* tRNA^{Gln}. The purified
812 isoacceptor tRNAs from the Δ*tgt* (light gray), Δ*arcS* (dark gray), and *TS559* (black) strains were
813 denatured in a background of 100mM NaCl with **A**) No $MgCL_2$, **B**) 100 µM $MgCl_2$, and **C**) 10 mM
814 $MgCl_2$.

815 **Figure 7**. Thermal denaturation profiles (1st derivative) of *in vitro* produced *T. kodakarensis*
816 tRNA^{Gln}(CUG). The data correspond to the unmodified tRNA transcript possessing G at position 15
817 (light grey), the modified transcript possessing $preQ_0$ (dark gray), and the modified transcript
818 possessing G^+ (black). The denaturing profiles were recorded in a background of 100mM NaCl with
819 **A**) no $MgCl_2$, **B**) 100 µM $MgCl_2$, and **C**) 10 mM $MgC1_2$.

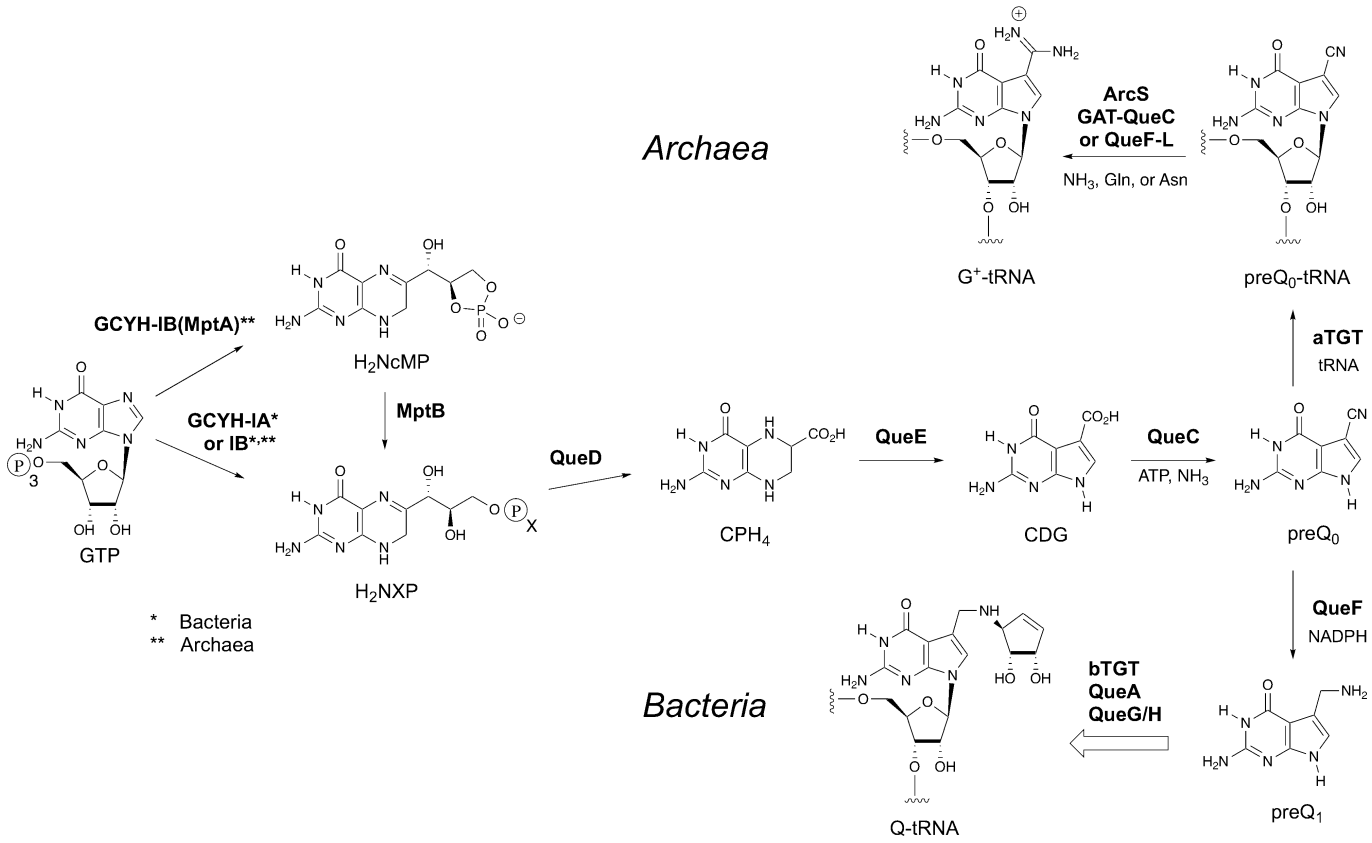
Archaea
Bacteria
GTP
GCYH-IB(MptA)**
GCYH-IA*
or IB*,**
H2NcMP
MptB
H2NXP
QueD
CPH4
QueE
CDG
QueC
ATP, NH3
preQ0
aTGT
tRNA
preQ0-tRNA
ArcS
GAT-QueC
or QueF-L
NH3, Gln, or Asn
G+-tRNA
QueF
NADPH
preQ1
bTGT
QueA
QueG/H
Q-tRNA
* Bacteria
** Archaea

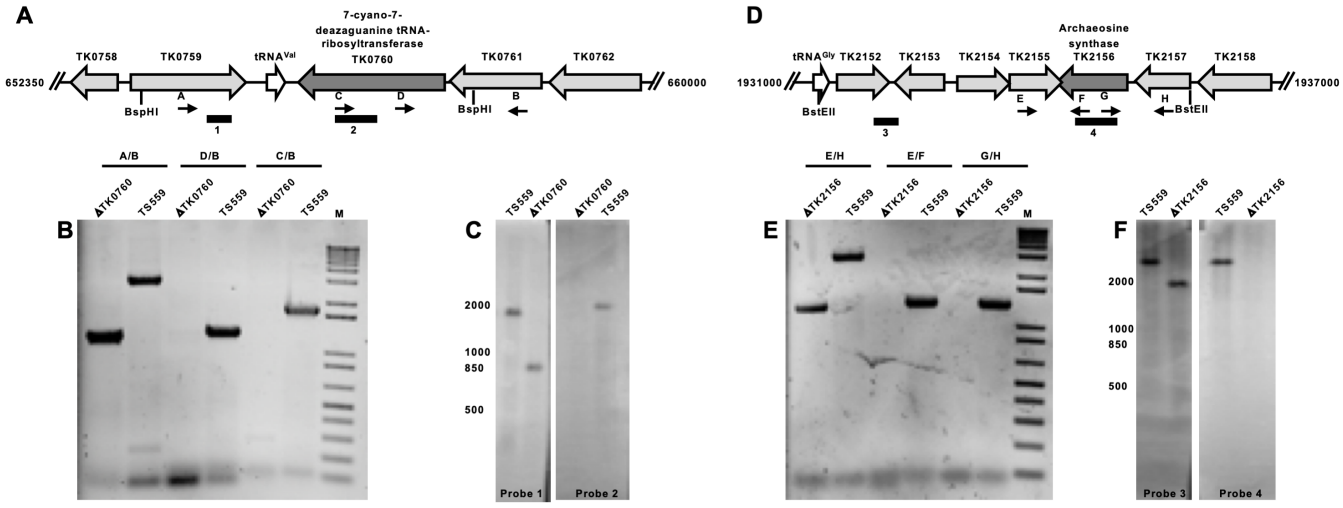
A
7-cyano-7-deazaguanine tRNA-ribosyltransferase TK0760
TK0758
TK0759
tRNA^Val
TK0761
TK0762
652350
660000
BspHI
BspHI
A
B
C
D
1
2
B
A/B
D/B
C/B
ΔTK0760
TS559
M
C
TS559
ΔTK0760
ΔTK0760
TS559
2000
1000
850
500
Probe 1
Probe 2
D
Archaeosine synthase TK2156
tRNA^Gly
TK2152
TK2153
TK2154
TK2155
TK2157
TK2158
1931000
1937000
BstEII
BstEII
E
F
G
H
3
4
E
E/H
E/F
G/H
ΔTK2156
TS559
M
F
TS559
ΔTK2156
TS559
ΔTK2156
2000
1000
850
500
Probe 3
Probe 4

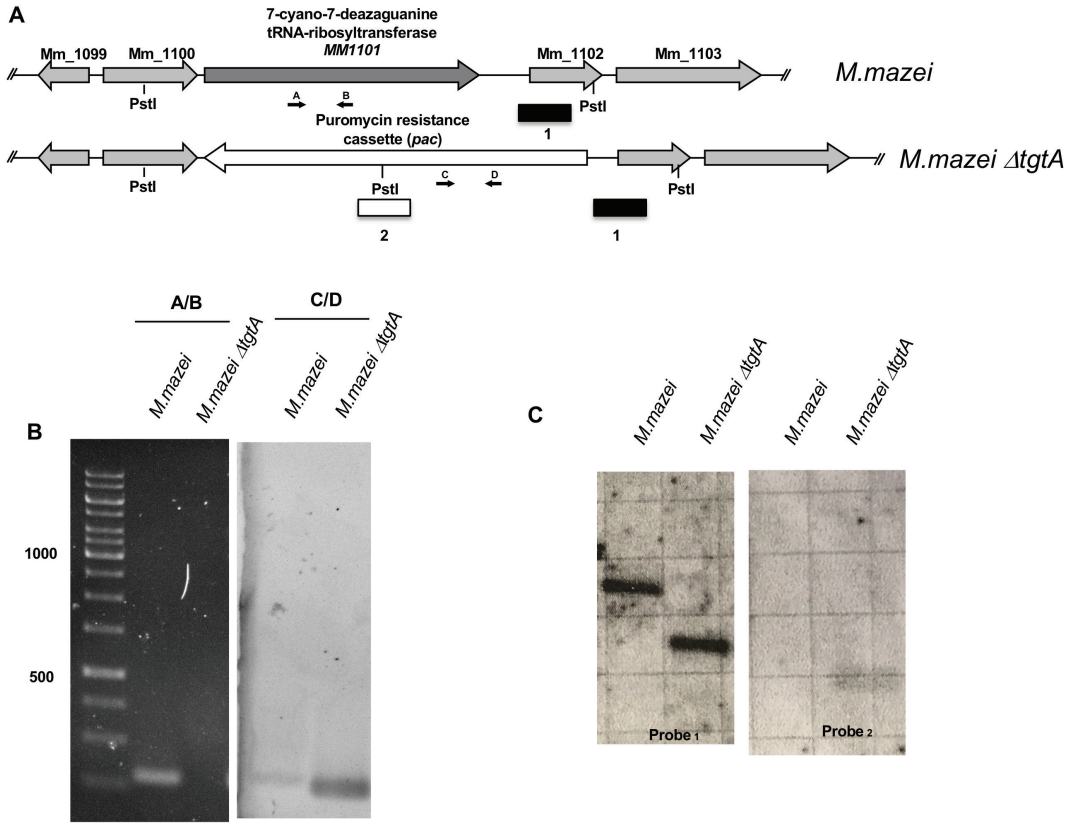
A
7-cyano-7-deazaguanine
tRNA-ribosyltransferase
MM1101
Mm_1099
Mm_1100
Mm_1102
Mm_1103
M.mazei
PstI
A
B
PstI
1
Puromycin resistance
cassette (pac)
M.mazei ΔtgtA
PstI
C
D
PstI
PstI
2
1
A/B
C/D
M.mazei
M.mazei ΔtgtA
M.mazei
M.mazei ΔtgtA
B
1000
500
C
M.mazei
M.mazei ΔtgtA
M.mazei
M.mazei ΔtgtA
Probe 1
Probe 2

Figure 3.

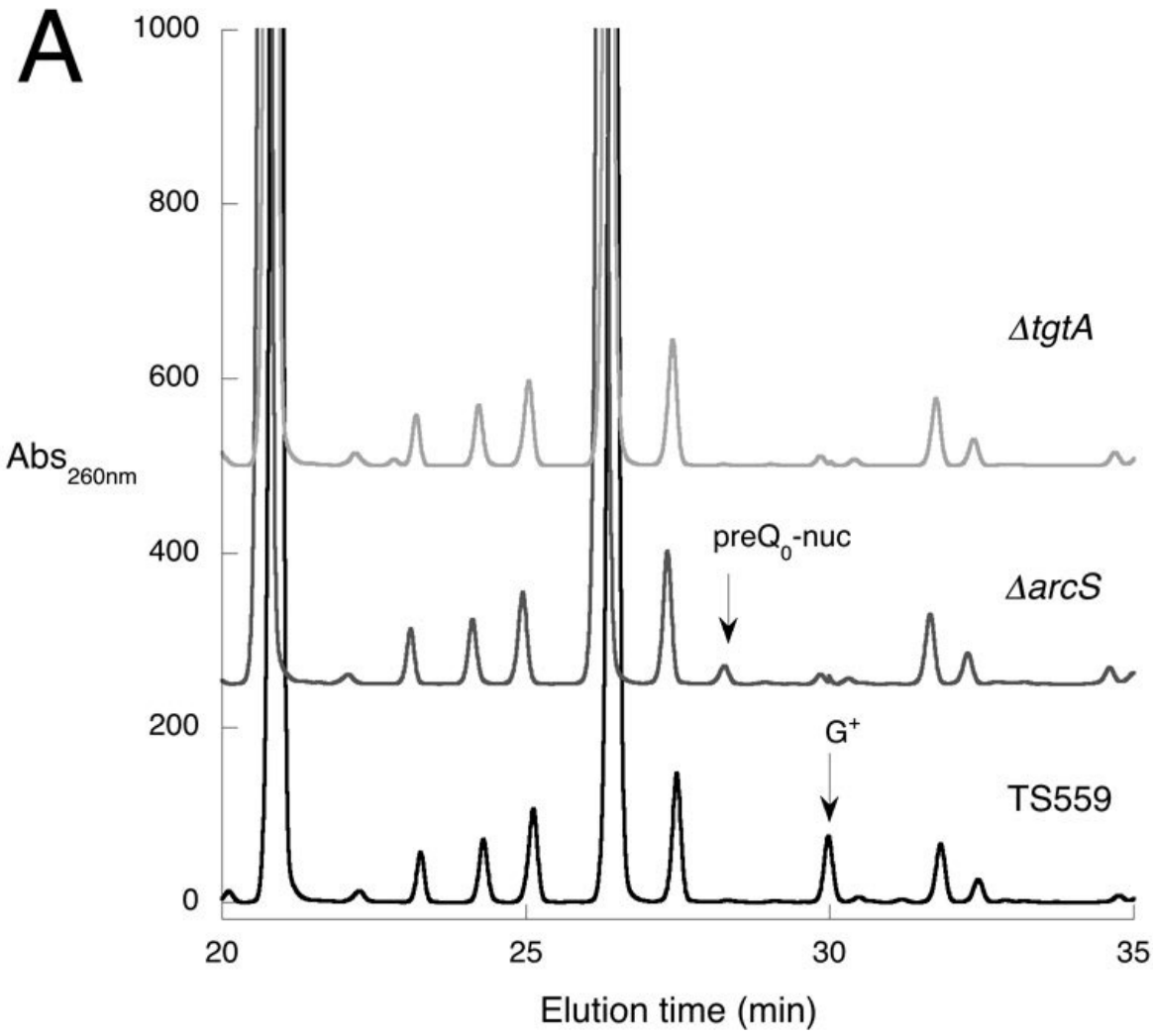
A
1000
800
600
400
200
0
Abs260nm
ΔtgtA
preQ0-nuc
ΔarcS
G+
TS559
20
25
30
35
Elution time (min)

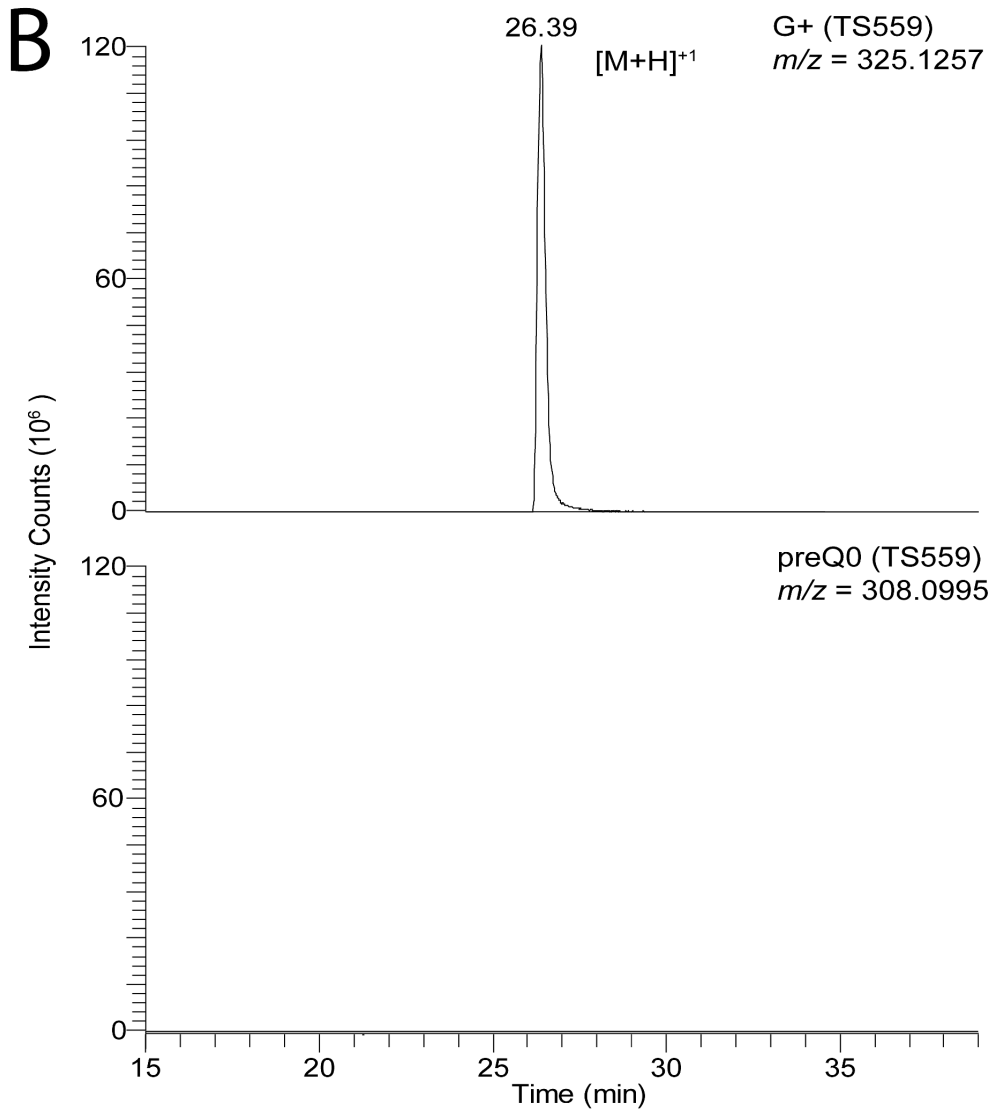
B
26.39
[M+H]+1
G+ (TS559)
m/z = 325.1257
120
60
0
Intensity Counts (10^6)
preQ0 (TS559)
m/z = 308.0995
120
60
0
15
20
25
30
35
Time (min)

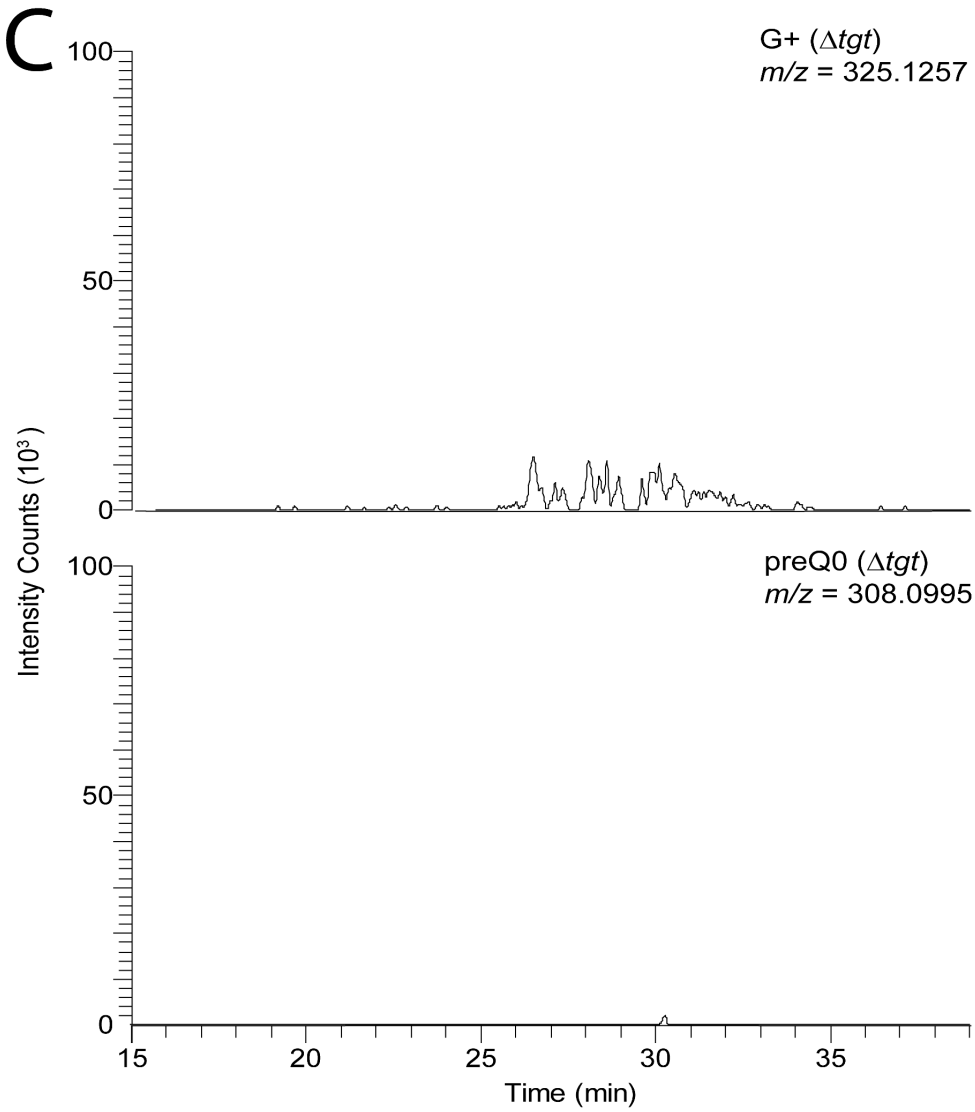
C
G+ (Δtgt)
m/z = 325.1257
preQ0 (Δtgt)
m/z = 308.0995
Intensity Counts (10³)
100
50
0
100
50
0
15
20
25
30
35
Time (min)

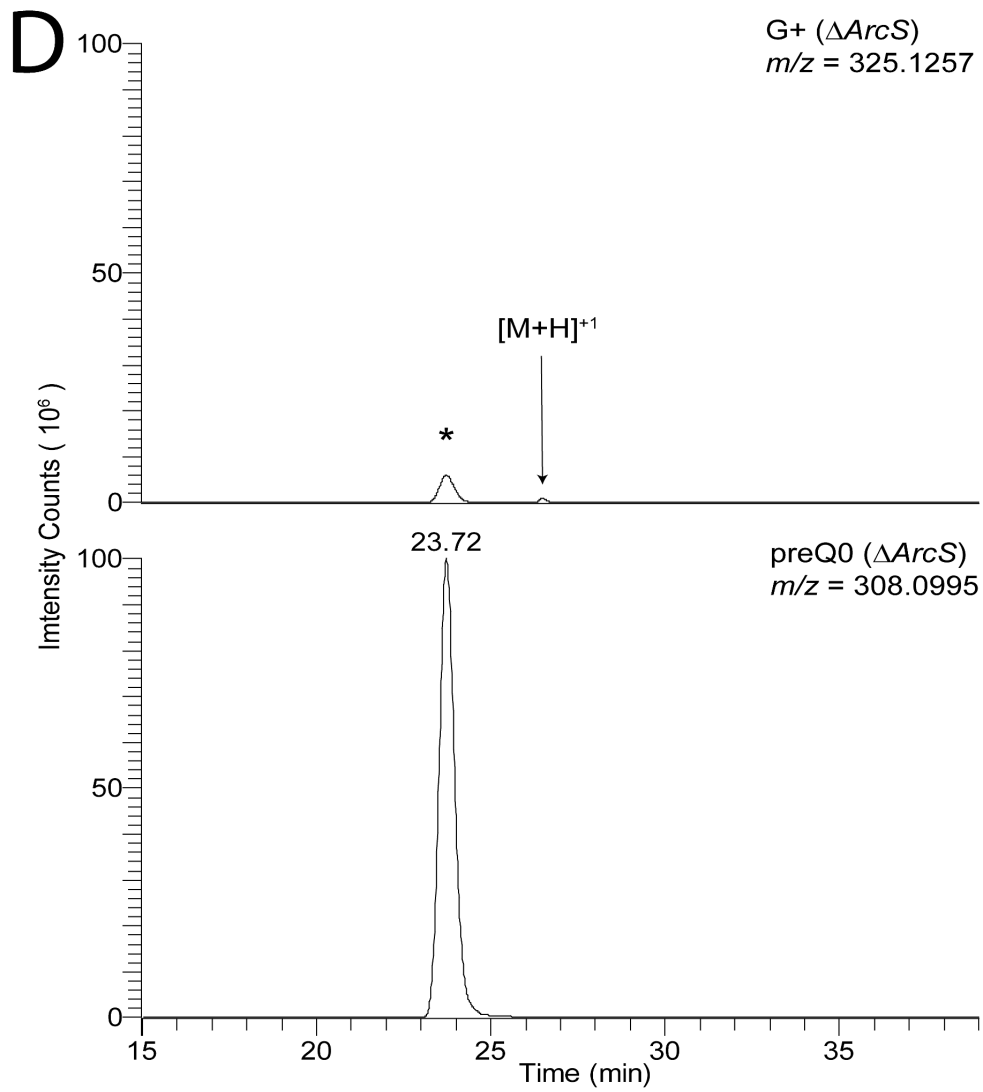
D
G+ (ΔArcS)
m/z = 325.1257
[M+H]+1
*
100
50
0
Imtensity Counts (10^6)
23.72
preQ0 (ΔArcS)
m/z = 308.0995
100
50
0
15
20
25
30
35
Time (min)

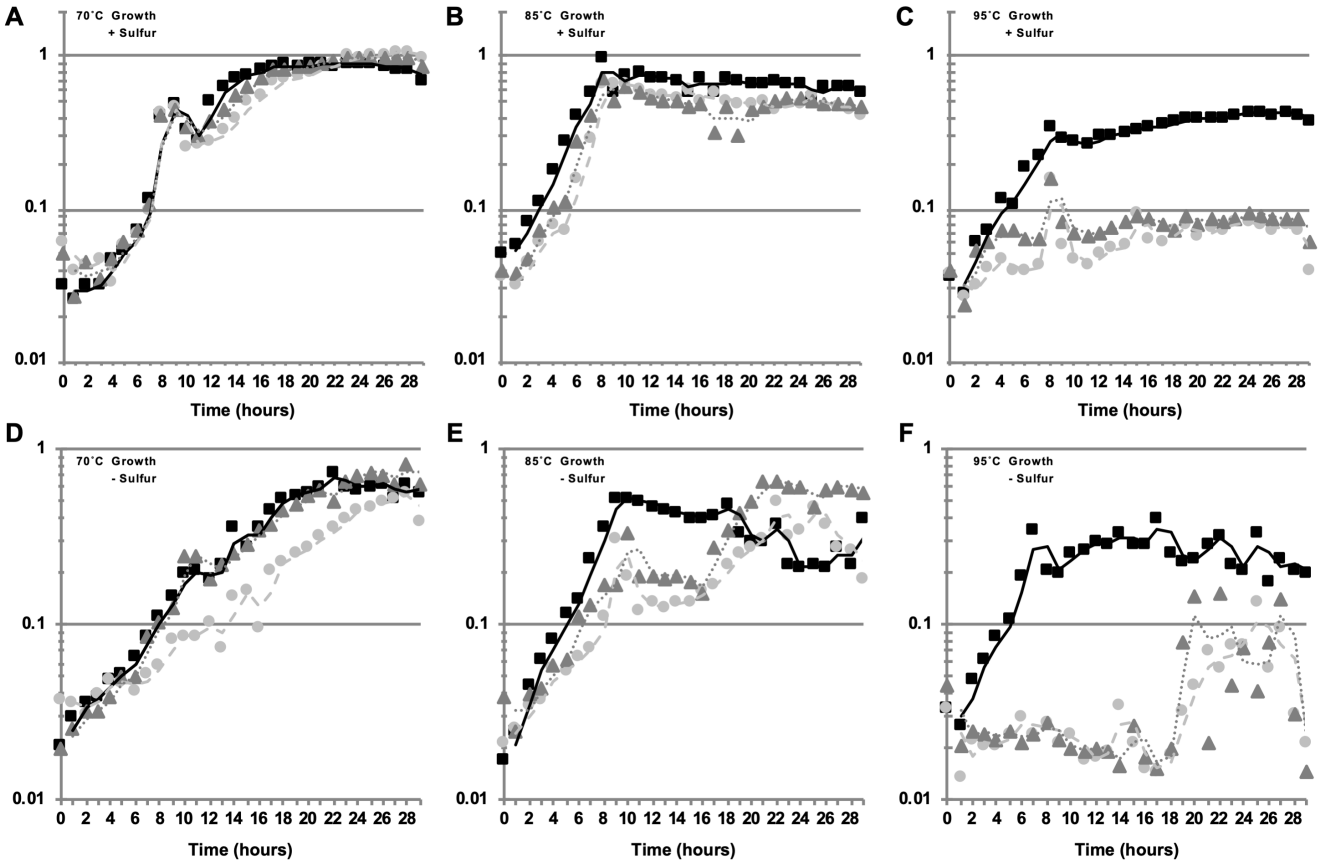
A
70˚C Growth
+ Sulfur
B
85˚C Growth
+ Sulfur
C
95˚C Growth
+ Sulfur
D
70˚C Growth
- Sulfur
E
85˚C Growth
- Sulfur
F
95˚C Growth
- Sulfur
1
0.1
0.01
0 2 4 6 8 10 12 14 16 18 20 22 24 26 28
Time (hours)

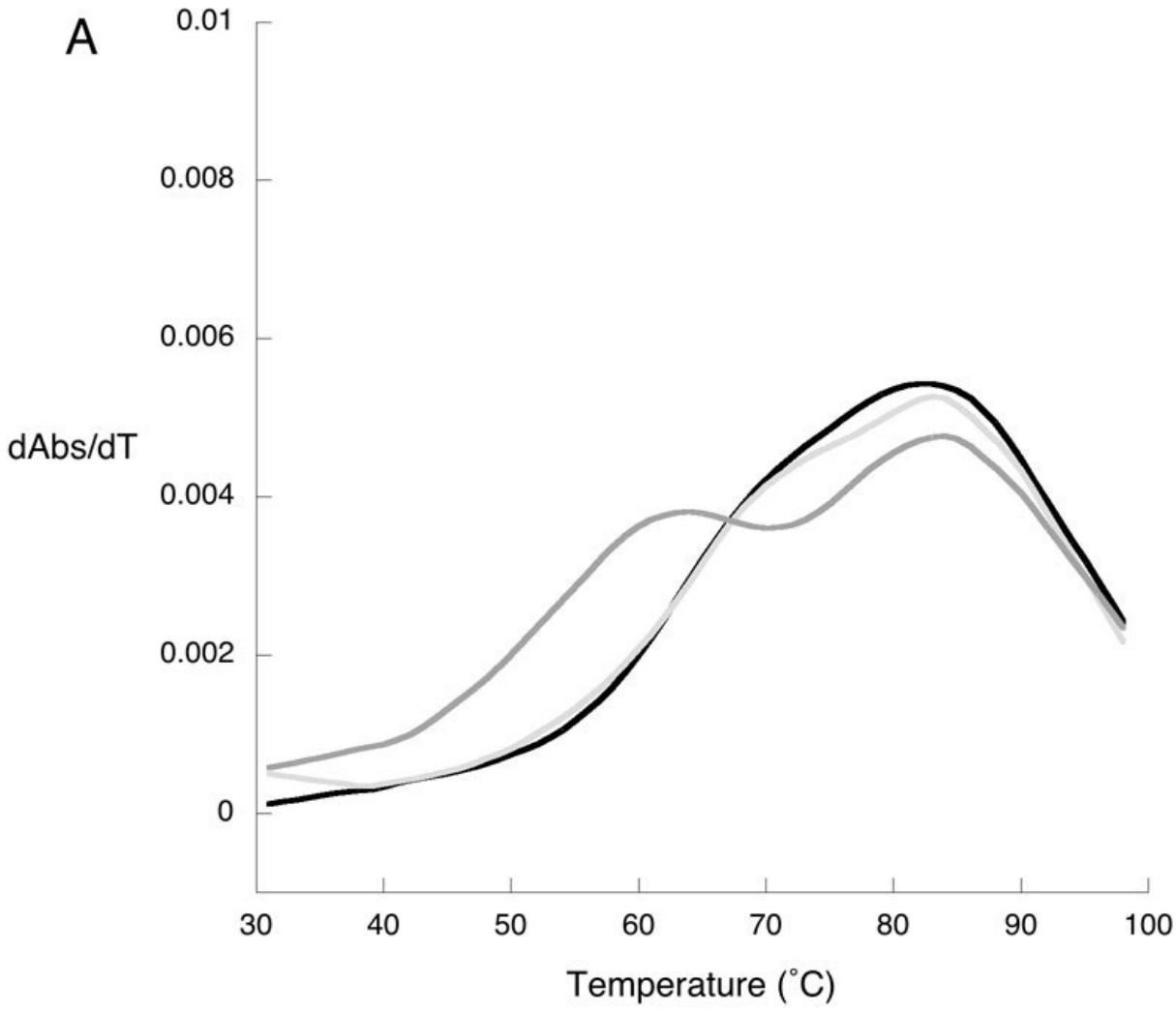
A
0.01
0.008
0.006
dAbs/dT
0.004
0.002
0
30
40
50
60
70
80
90
100
Temperature (˚C)

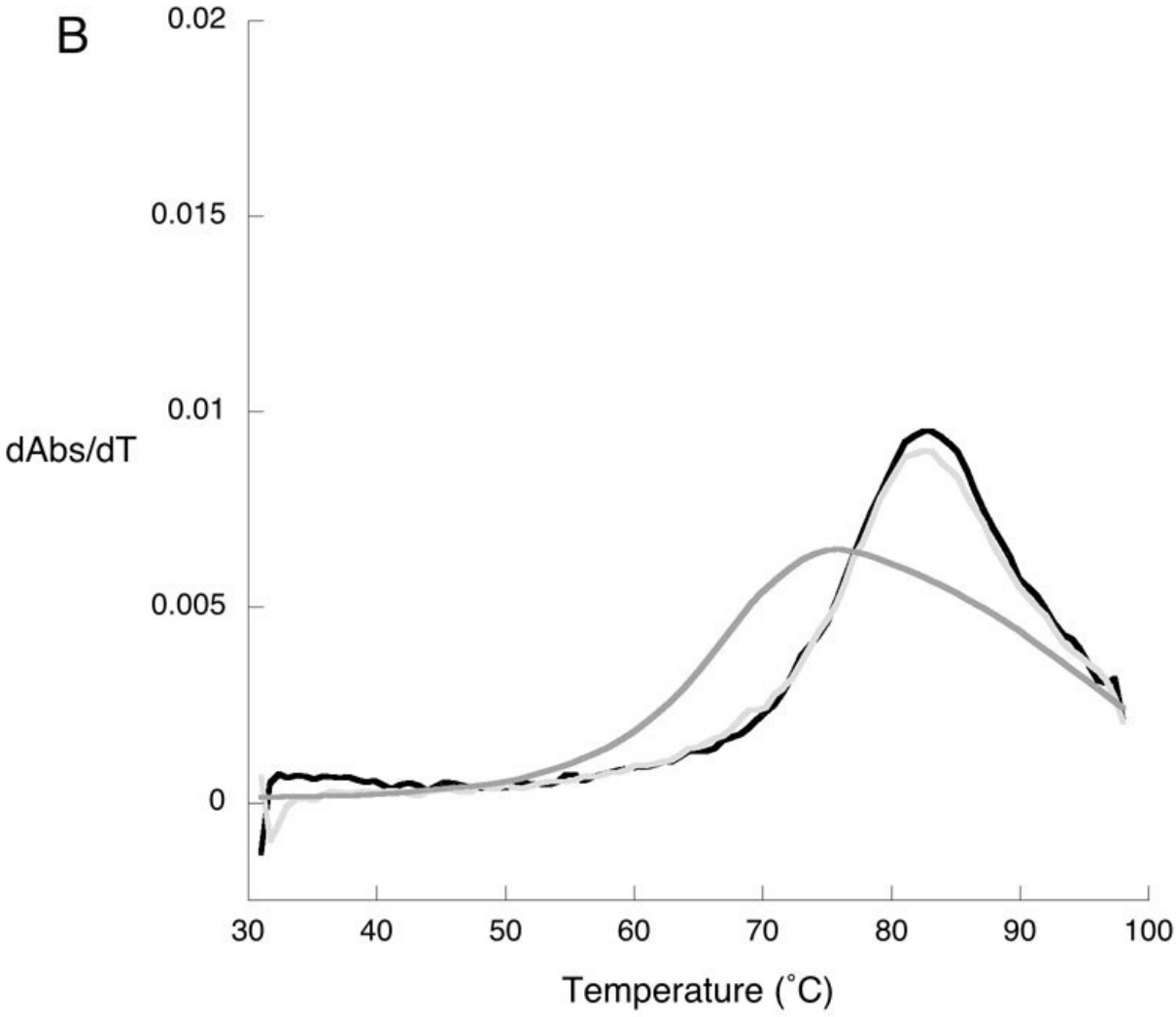
B
0.02
0.015
0.01
0.005
0
dAbs/dT
30
40
50
60
70
80
90
100
Temperature (˚C)

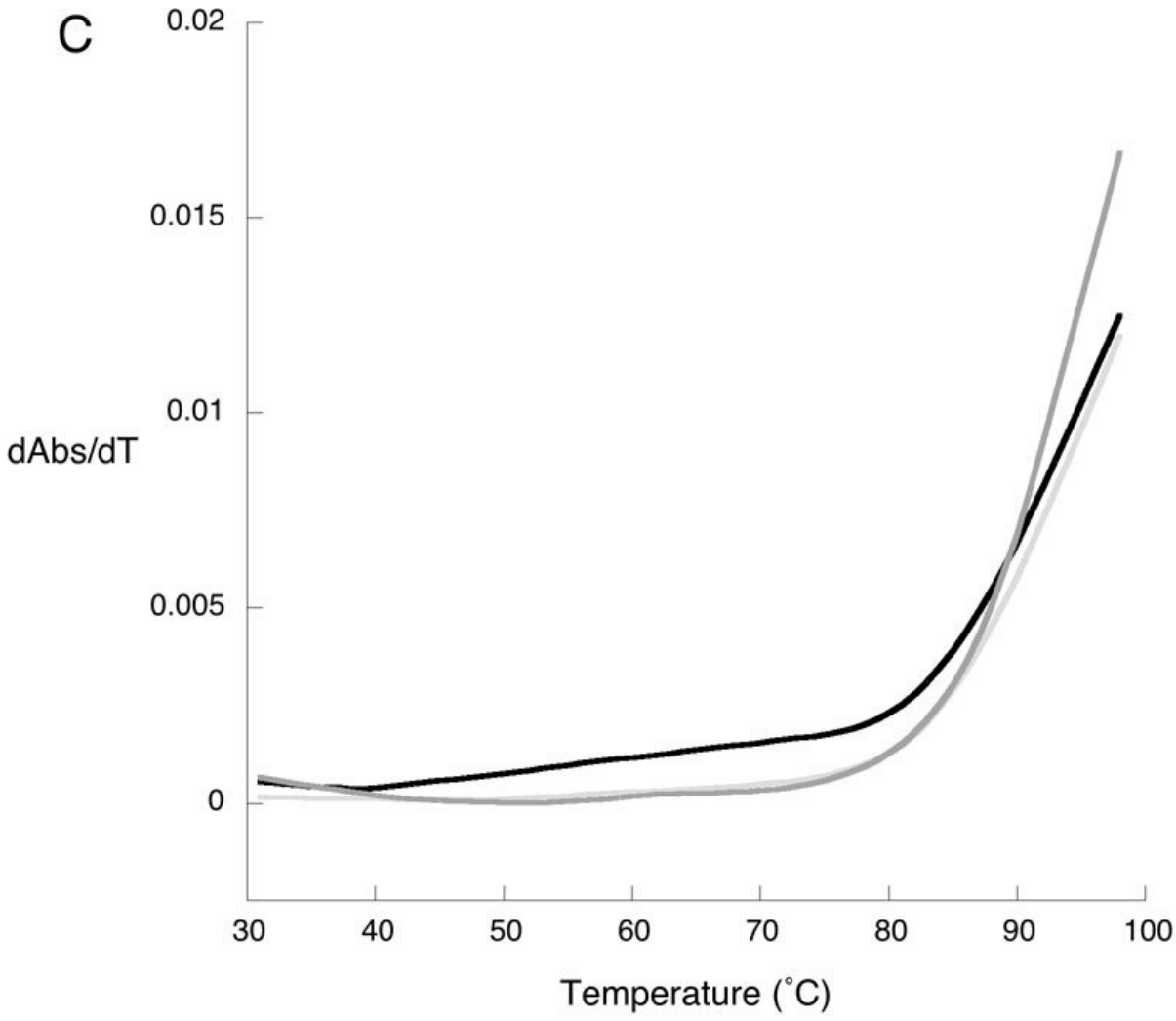
C
0.02
0.015
0.01
0.005
0
dAbs/dT
30
40
50
60
70
80
90
100
Temperature (˚C)

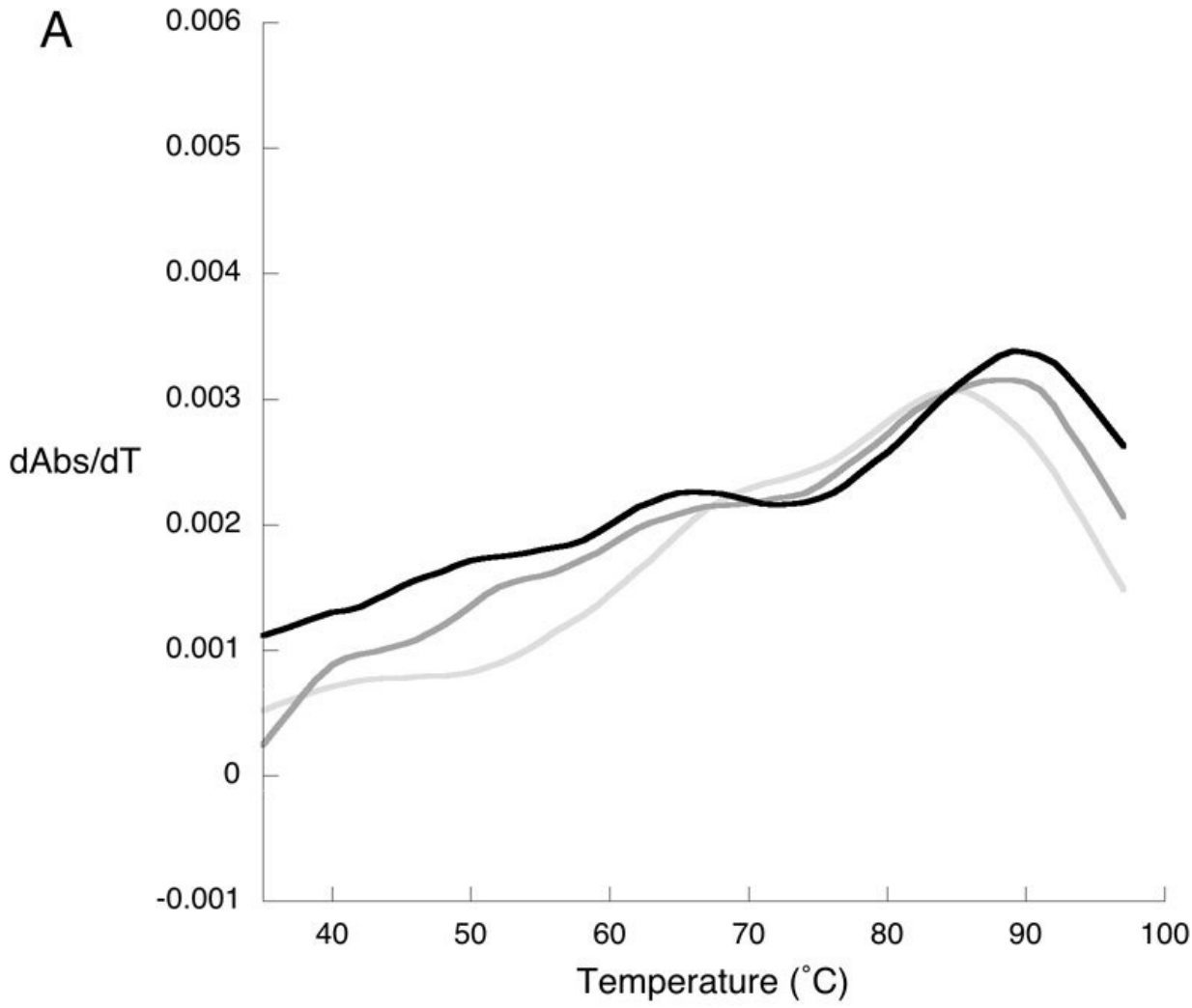
A
0.006
0.005
0.004
0.003
0.002
0.001
0
-0.001
dAbs/dT
40
50
60
70
80
90
100
Temperature (˚C)

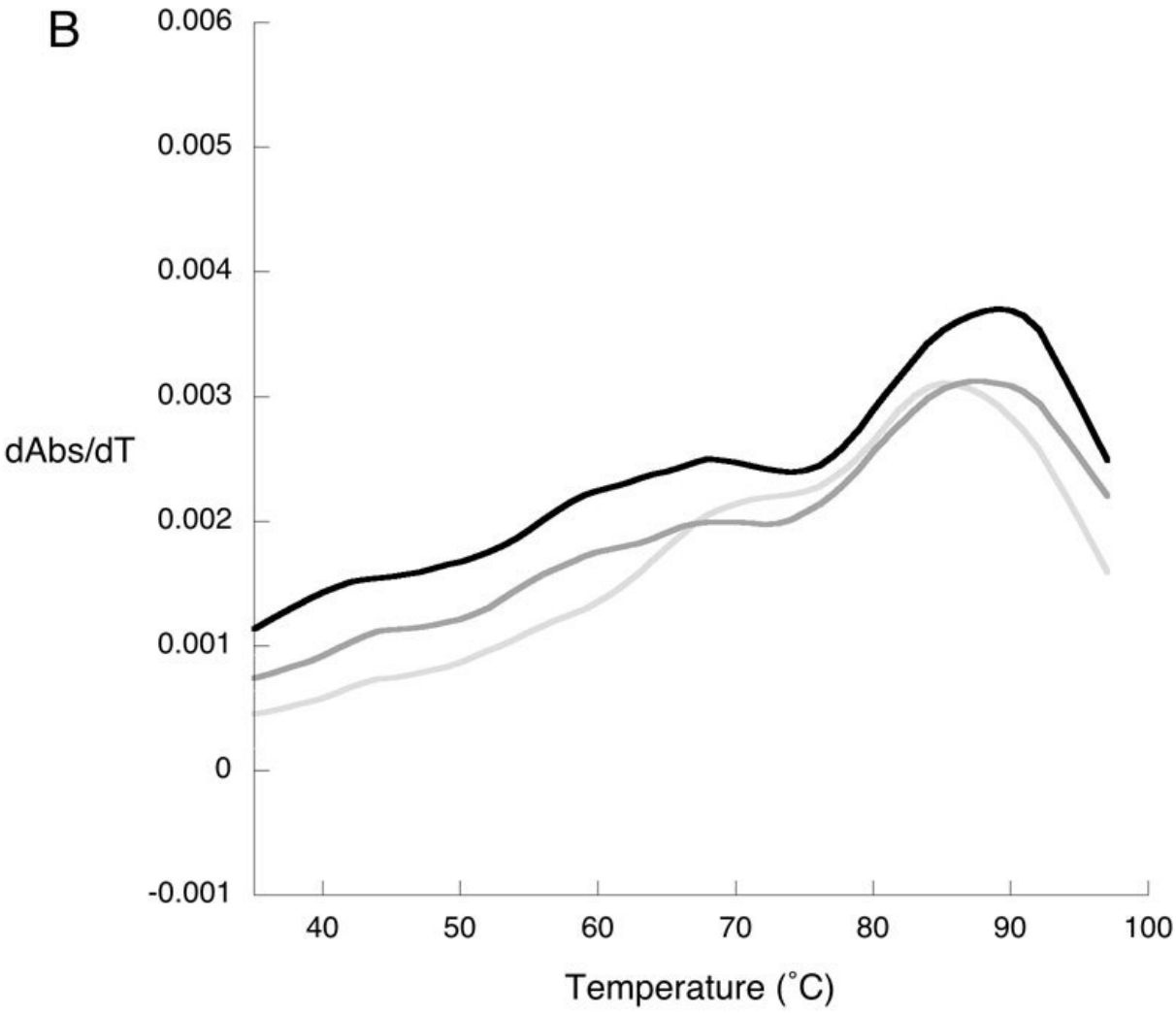
B
0.006
0.005
0.004
0.003
0.002
0.001
0
-0.001
dAbs/dT
40
50
60
70
80
90
100
Temperature (˚C)

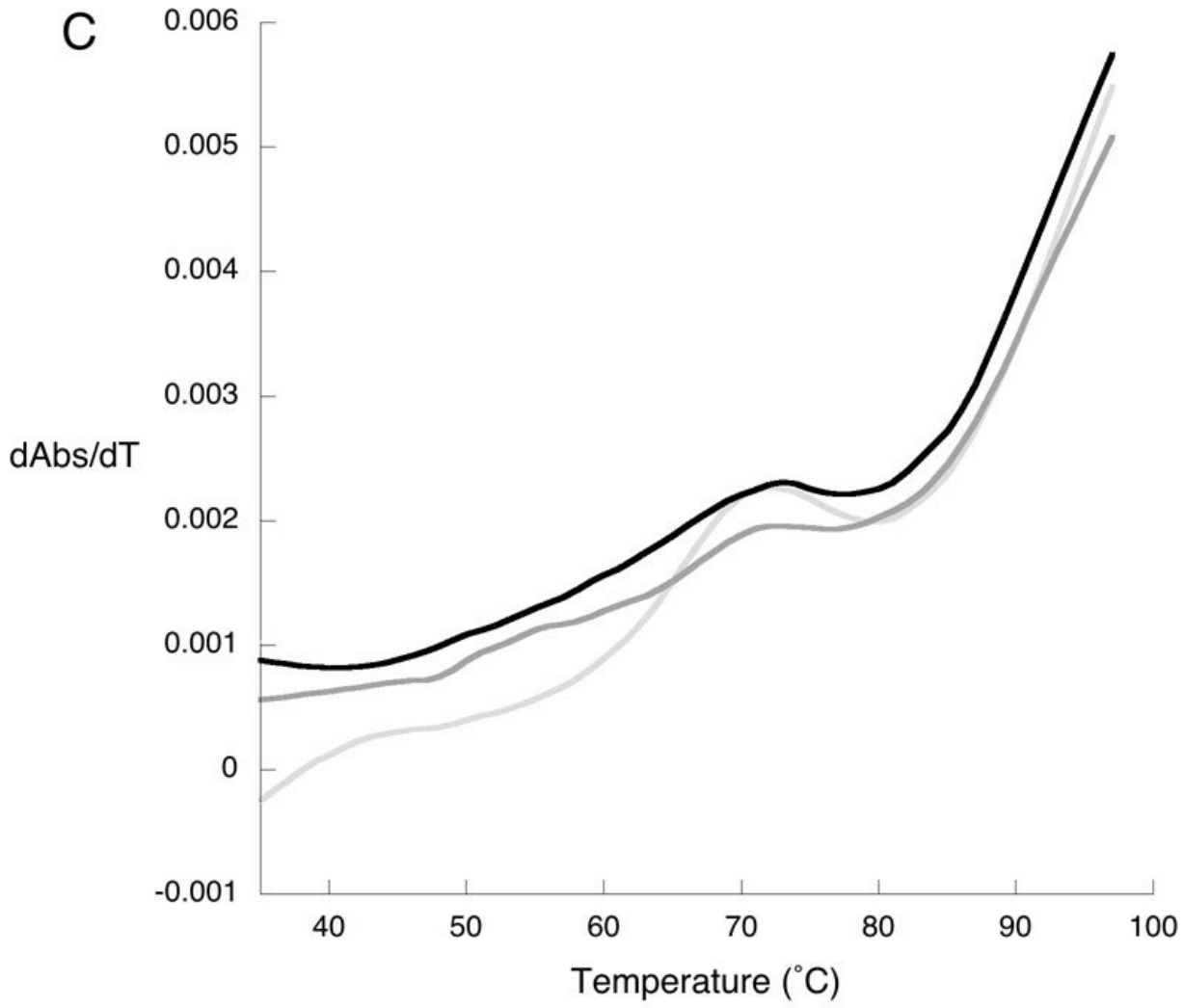
C
0.006
0.005
0.004
0.003
dAbs/dT
0.002
0.001
0
-0.001
40
50
60
70
80
90
100
Temperature (˚C)